Polydopamine and Polydopamine-Glutaraldehyde Materials; Film and Particle Synthesis, Surface Modification, and Varying Behavior in an Optical Trap

Andrew J. Nuhaily

A thesis
submitted in partial fulfilment of the
requirements for the degree of

Master of Science

University of Washington

Summer 2023

Committee:

Peter J. Pauzauskie

Eleftheria Roumeli

Program Authorized to Offer Degree:

Materials Science and Engineering

University of Washington

Abstract

Polydopamine and

Polydopamine-Glutaraldehyde Materials;

Film and Particle Synthesis,

Surface Modification, and

Varying Behavior in an Optical Trap

Andrew J. Nuhaily

Chair of the Supervisory Committee:

Peter J. Pauzauskie

Materials Science and Engineering

Materials derived from polydopamine are multifunctional and it is easily deposited on many surfaces because of highly reactive amine and indole chemistry. The structure of dopamine confers it both negative and positive moieties and materials derived from it are enabled by a great deal more available surface chemistries than other materials that only possess one. The ceramic surfaces from the trials in this thesis were found to not readily accept PDA deposition. By comparison, charged surfaces such as glass, metals, and plastics, easily interact with this flexible monomer.

PDA is made from dopamine monomers and downstream oligomers. During synthesis, it conforms to surfaces and can completely envelop charged or metallic substrates. In this thesis, Y/Yb-doped ceramic crystals were uniformly coated using mole fraction excess concepts of Le Châtelier's Principle. By adding an excess of monomer, the formation of nanospheres is made

less favorable and films grow, instead. In response to downstream attempted enzyme conjugation, the uniform coating irreversibly aggregated.

To improve chemical resistance, crosslinked versions of these coats were developed using glutaraldehyde and hydrothermal pressure to forcibly deposit a coating of polydopamine crosslinked by glutaraldehyde (PDAG). This polymer is stable in the presence of PBS and is therefore a good candidate for developing bioactive or corrosion-resistance applications for coated ceramics and possibly metals.

PDA nanoparticles are able to be controllably aggregated/dispersed against a glass cover slip in a 1020nm optical trap are able whereas PDAG particles made via hydrothermal methods show differing interactions with the laser beam. These two particle types may be viable candidates for exploration in Brownian motion studies or possibly in the production of NV^- diamond nanoparticles.

1. Introduction

For the last year or so, I have studied how dopamine can be polymerized to coat surfaces that are, at the time of this writing, believed to be electrostatically neutral. These are ceramic surfaces composed of Yttrium/Ytterbium Lithium Fluoride (YLF) and beta-phase Sodium Yttrium/Ytterbium Fluoride (β-NaYF). These doped ceramics have the capacity to be laser cooled at 1020nm and are intended to be used to study certain enzymatic rate kinetics via radiative cooling mechanisms. Additionally, it may be possible to utilize them to transition certain biotechnological methods from convection heating/cooling to rapid optical methods.

The spreading of dopamine over these materials is novel work because a great deal of research that has been done with polydopamine (PDA) has involved the coating of a charged surface. From these works, the reactive groups will be identified, the polymeric bonding pathways detailed, and advanced surface mechanics recognized for several applications. Common coating mechanisms are dip coating [1], electroplating [2], and (very generally) stirring

at standard temperature and pressure for extended time under basic conditions [3]. In the time spent reading and analyzing the works of others, I found that not much work has been done regarding the hydrothermal synthesis of PDA and what, if any, effect pressure has on the formation of polydopamine nanospheres which, even by themselves, have powerful biomedical application [4].

The goal of this thesis was to develop a method by which to seed a nanofilm of PDA on a sample of rare-earth (RE)-doped ceramic microparticles. The first “success” was seen using YLF (Yttrium/Ytterbium Lithium Fluoride) crystals. The downstream work (enzyme conjugation to the surface) was rendered seemingly impossible due to more favorable chemical interactions. These interactions, essentially, “tore off” this uniform coat and condensed it into something of a slag that still, remarkably, showed an active response to the assay the coating was being engineered for.

It can be difficult to recognize success in research because some successes objectively appear to be failures. During my undergraduate research, I learned that the hallmark of success is the quality of information obtained from any measured moment. For what this thesis concerns, this means that yes, at one point, the particle was completely coated. No, it was not a uniform coat. It was bumpy and forms of PDA other than the film were present. Yes, the coating did come off in downstream work. But surprisingly, no, the coating did not completely separate from the ceramic particle. Finally, yes, the results of antibody conjugation showed activity in the assay that was being studied for unpublished rate kinetics research.

All research comes from the spark of motivation. To theorize in polymer chemistry, one must consider very outlandish outcomes within a synthetic system. If the conditions for a polymer species to form are satisfied, a polymer species will direct its own formation (a whole field of study, itself). For even the most minute structure, it will always come into existence even if the duration is incredibly short (unless the system is specifically controlled against its

formation). For dopamine and its downstream oligomer species, all must exist throughout the oxidation of dopamine as PDA materials or structures adhere, grow, and/or nucleate. This brings this thesis to its main point and question: How is it possible to conjugate an enzyme to an accepting surface that physically altered by the reaction conditions necessary for conjugation? The answer applied here was polymer cross-linking.

1.1 The Chemistry of Polydopamine

Polydopamine materials were first reported in 2007 [1] and have since been explored in a wide variety of applications. They have been characterized extensively and it has been shown that reaction conditions can selectively produce functional groups on the surface of the formed PDA. The reactive sites of dopamine (**Figure 1)** can be broken down into base parts: a catechol unit prone to oxidation to o-quinone and a primary amine. These reactive molecular species are additionally able to reduce metals and are used in secretions produced by mussels and sand worms as coacervates (fluid-fluid phase-separation due to charge interactions while in electrically-neutral pH) to seek out and quickly spread over a substrate underwater by rapidly spreading and reducing metal ions to “sticky.” [5]

1.1.1 Brief History of Dopamine Chemistry in Polydopamine Research

The following several figures display the oxidation of dopamine originally considered for the formation of polydopamine. This pathway implies that from dopaquinone, the formation of L-dopa establishes an oxidative potential to form many intermediate catechol and amine-containing species- as shown in **Figure 2**. From this scheme, it was believed that these intermediate pathways terminate in the formation of eumelanin species (e.g. like the skin pigment). The monomer units for these eumelanin precursors are shown in **Figure 3** and their expression can be recognized in the classical eumelanin structure found in **Figure 4.**

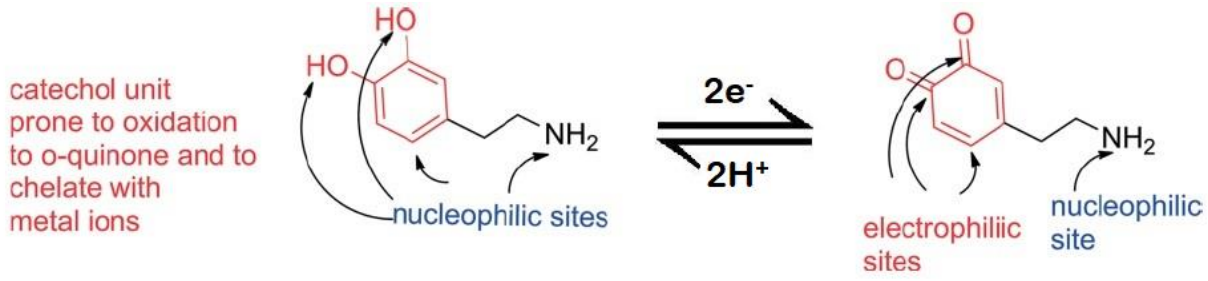

Figure 1. Nucleophilic (blue) and electrophilic (red) redox sites of dopamine (left) and dopamine-o-quinone (right) [6]

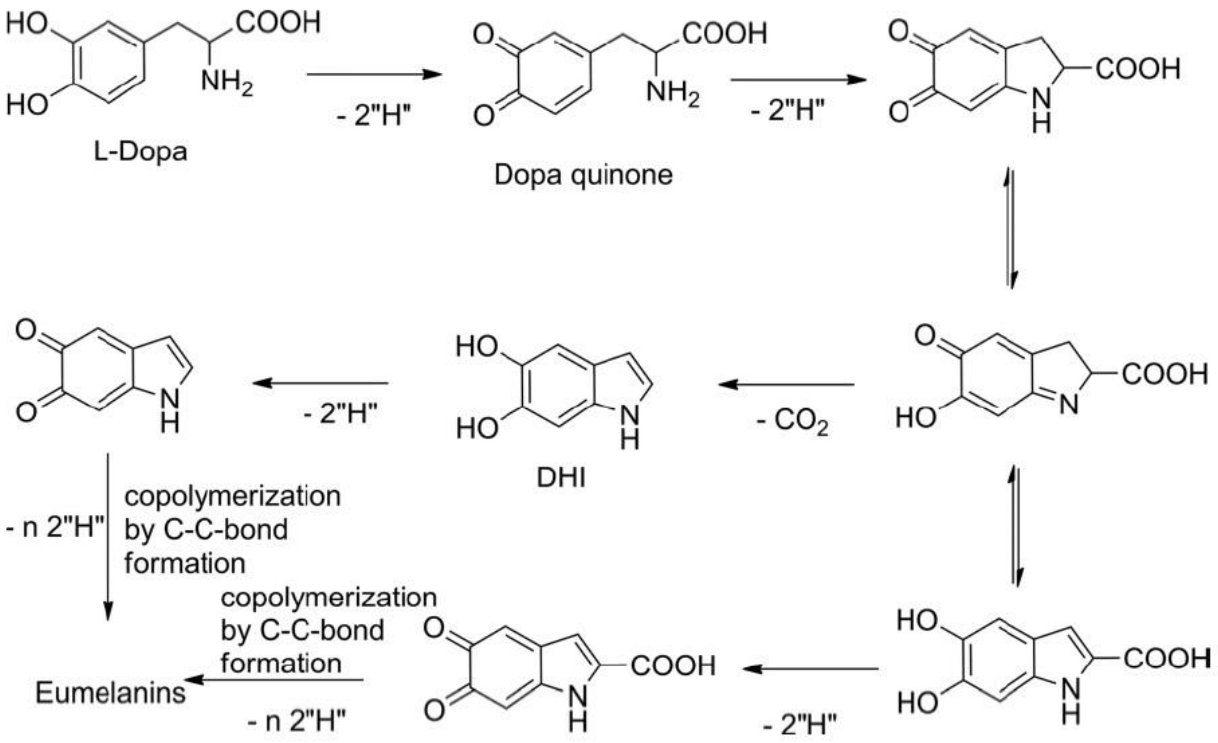

Figure 2. Raper-Mason Scheme for formation of L-Dopa intermediates throughout oxidative formation of eumelanin species. [6]

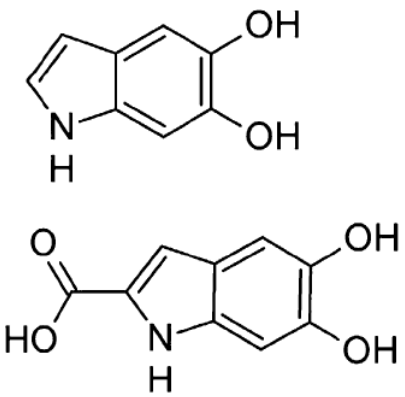

Figure 3.

Structure of eumelanin monomers 5,6-dihydroxyindole (DHI, top) and 5,6-dihydroxyindole-2-carboxylic acid (DHICA, bottom) [8].

Figure 4.

Classical model of eumelanin structure. Careful observation recognizes a large number of indolic compounds such as DHI (**U1**) and DHICA (**U2**). Other monomer species derivative of L-dopaquinone include 5,6-indolequinone (IQ, **U3**), L-dopamine (**U4**), and carboxylated pyrroles (**U5**). Structural arrows correspond to sites susceptible to polymeric growth. [7]

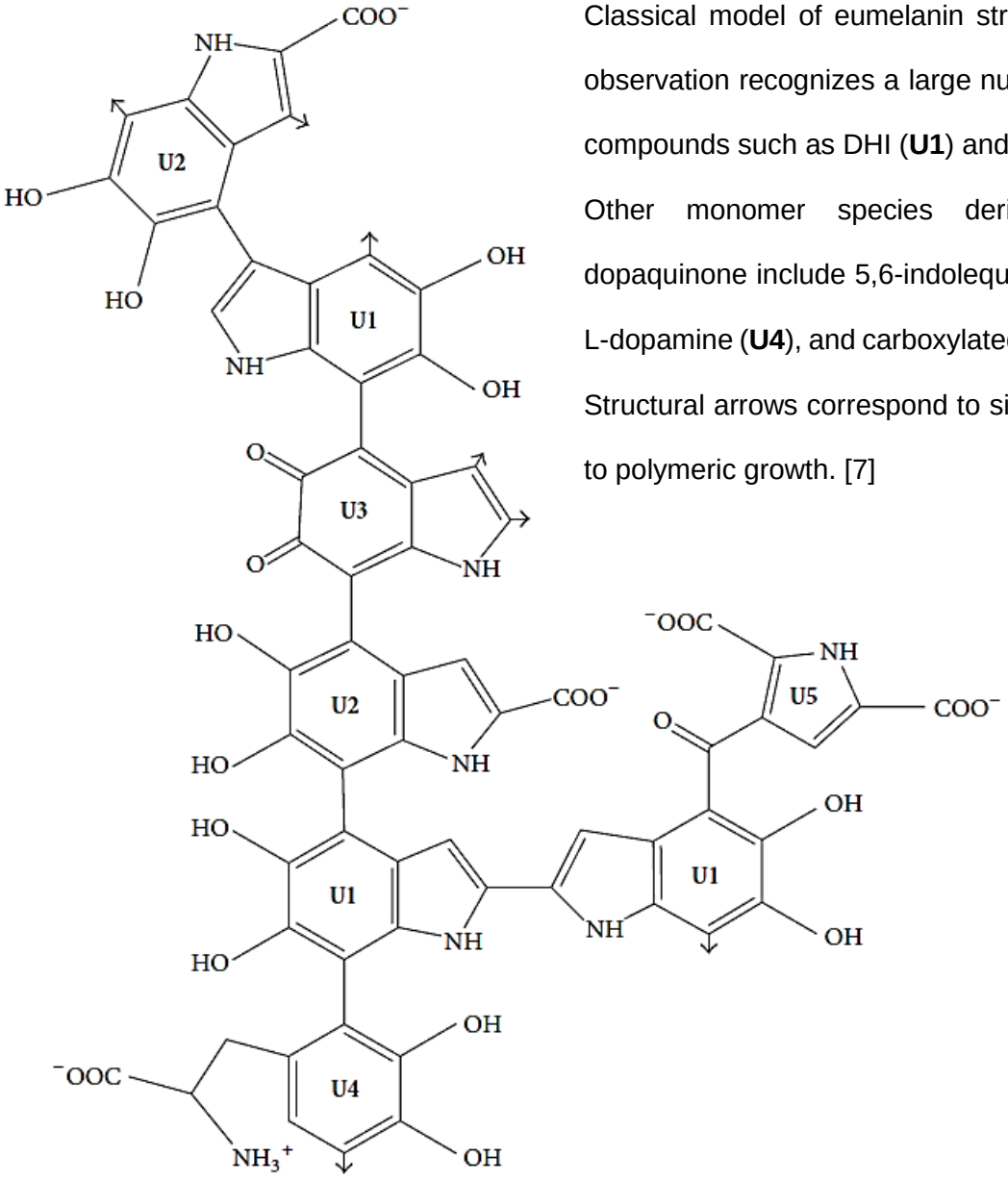

While this may be a viable pathway for eumelanin synthesis in the human body, it had previously been found that different products would form when using DHI as a precursor instead of DA [9]. Various analytical methods were used to delve deeper into PDA composition. Using solid NMR, mass spectroscopy, X-ray crystallography, FTIR spectroscopy, UV/Vis spectroscopy, AFM, and chemical degradation, the case was presented that PDA is a mixture of oligomers (with trimers and tetramers in abundance) composed of monomers. Several species proposed on the basis of MS and NMR are shown in **Figure 5**. The monomer units for PDA are shown in **Figure 6** which displays the general monomer composition from highest abundance at the top to less abundant pyrrolecarboxylate units at the bottom (these are considered to form due to oxidative degradation of indole quinone by hydrogen peroxide generated during oxidation). It is fundamental to note that zwitterionic tautomers exist in this scheme and may

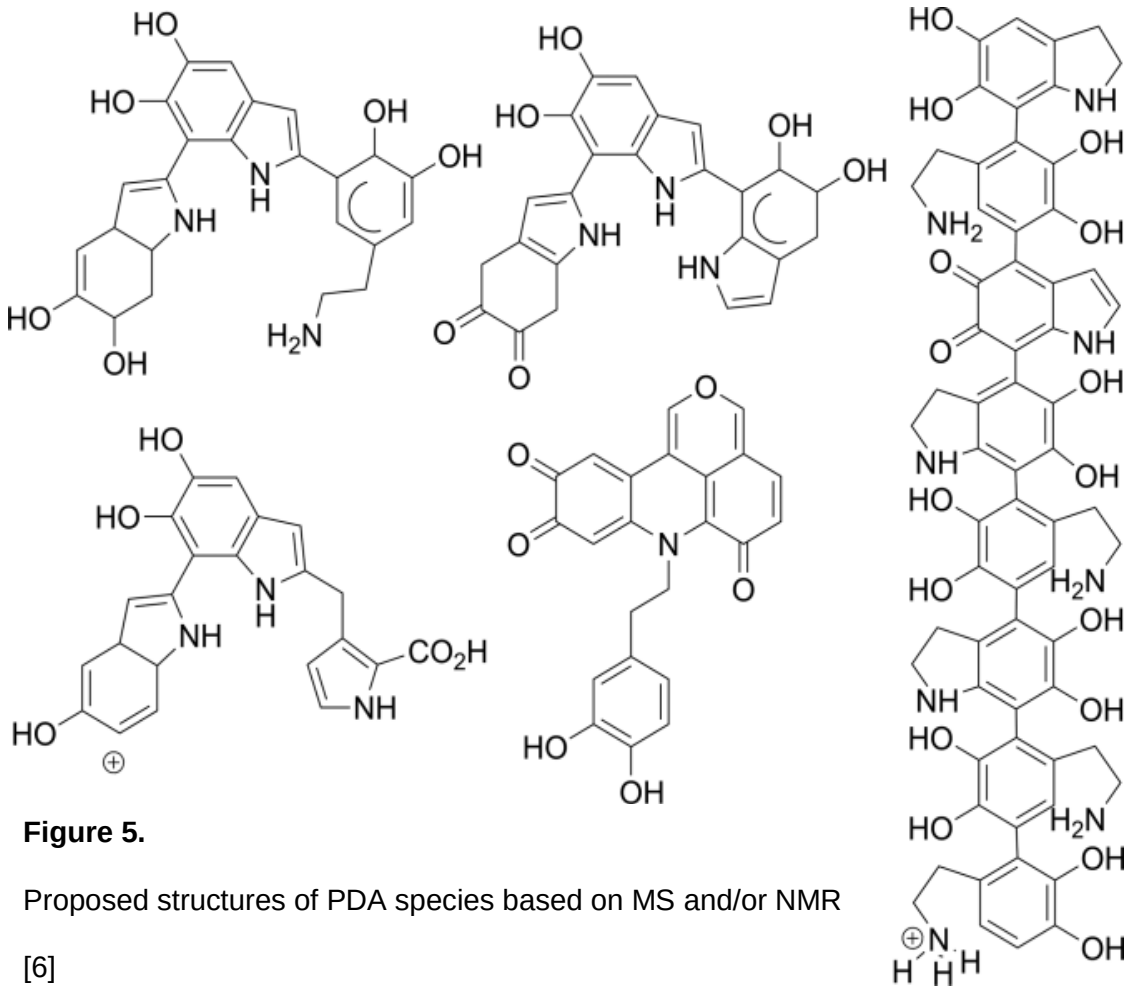

Figure 5.

Proposed structures of PDA species based on MS and/or NMR [6]

explain the formation of supramolecular structures by H-bonding, π-π interactions, and cation-π interactions. [6]

1.2 Background – Surface-level Polymer Synthesis in Dopamine

1.2.1 Polydopamine Synthesis

Recalling the redox activity from **Figure 1**, the chemical potential of the monomers shown in **Figure 6** is recognizable**.** Surprisingly, there was a measure of debate of what physical mechanism by which DA self-organizes into higher-order structures. This mechanism is a particular thing to consider as DA oxidation produces polymeric materials in a variety of geometries, including: monodisperse spheres [4], hollow or template shells [10], and surface-conforming films [11].

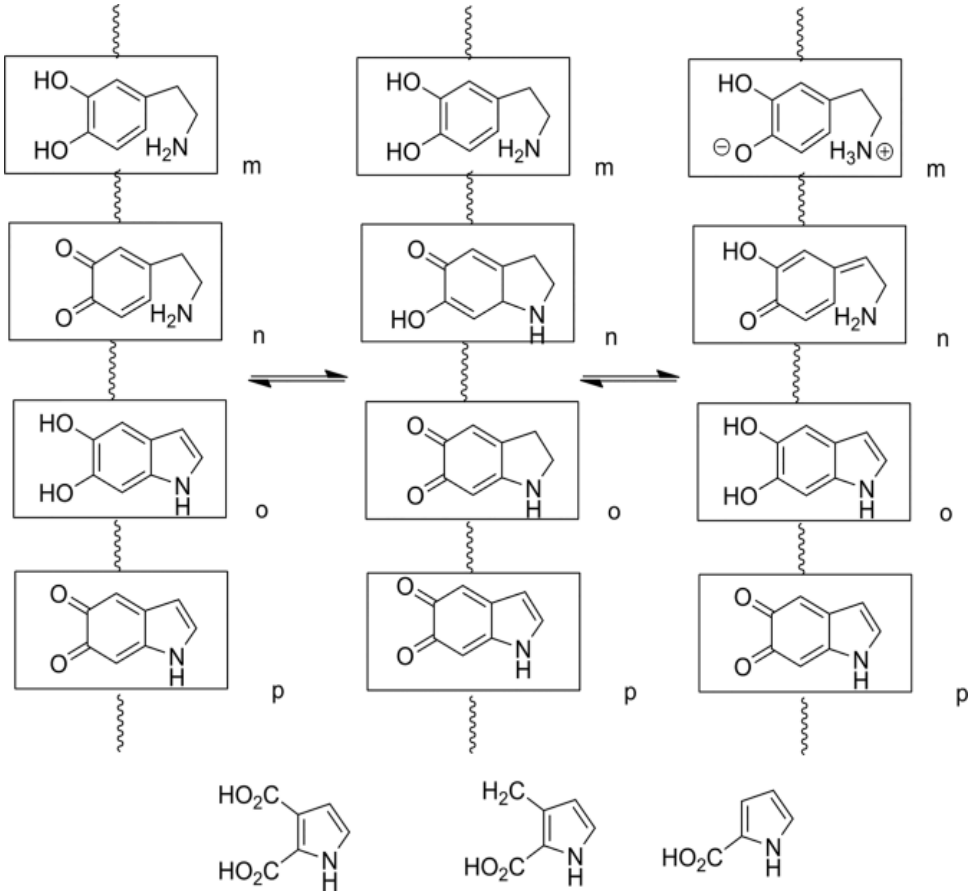

Figure 6.

Proposed general structures of PDA monomers (m, n, o, p) and less abundant pyrrolecarboxylate units at the bottom. Zwitterionic species can be noted in the right column. Pyrrolecarboxylate species are expected to form as a result chemical degradation by H_2O_2 formed due oxidative conditions [6]

The potential of PDA surfaces has sparked a great deal of research they are able to satisfy many application criteria such as being bioactive/biocompatible [4], maintaining adhesive behavior while in aqueous and other solvent conditions [5], being conductive [12], and having strong optical responses [11]. It is crucial to consider how the chosen synthesis process affects the final product. For size dependency, polydopamine nanosphere diameter can depend on the concentration of dopamine, the molar ratio of ammonia to dopamine (often simply regarded as the pH) [4], and/or the amount of heat in the reaction. For the rate of polydopamine formation, metal cations [6, 14] and buffers such as Tris, PBS, and bicarbonate [13] can be used- even in acidic conditions- and still produce PDA materials. Lastly, this point about how polydopamine formation can occur more readily in buffer is one of the pillars upon which this thesis was written so it must be openly discussed.

1.2.2 PDA Behavior in Buffered Solutions (Tris, PBS, Bicarbonate) [13]

What takes roughly 25 hours to produce via aqueous oxidation only takes up to a few hours when instead using buffers such as Tris (tris(hydroxymethyl)aminomethane), PBS (NaH_2PO_4, Phosphate-Buffered Saline), or bicarb ($NaHCO_3$, Bicarbonate buffer). This comes with a few caveats which is why it was mostly excluded from the procedure of film formation in this research body. The first caveat is that the units of buffer may participate as covalent modifiers within the polymer structure, as is shown to be done with Tris (**Figure 7**). This ultimately produces a material coat with functional groups that differ slightly from oxidative polymerization. With downstream antibody conjugation utilizing PBS, it was observed that the complete film coating would irrevocably aggregate- leading to the next caveat.

As was mentioned previously, unless it is specifically controlled to not be produced, a polymer species must always be assumed to come into existence- even if only for a short time. Speaking in terms of polydopamine synthesis via oxidation, unless the redox groups that PBS targets become unavailable, the PDA coating will never be safe from this aggregation behavior. This is principally because the extent to which polydopamine oligomers polymerize solely under

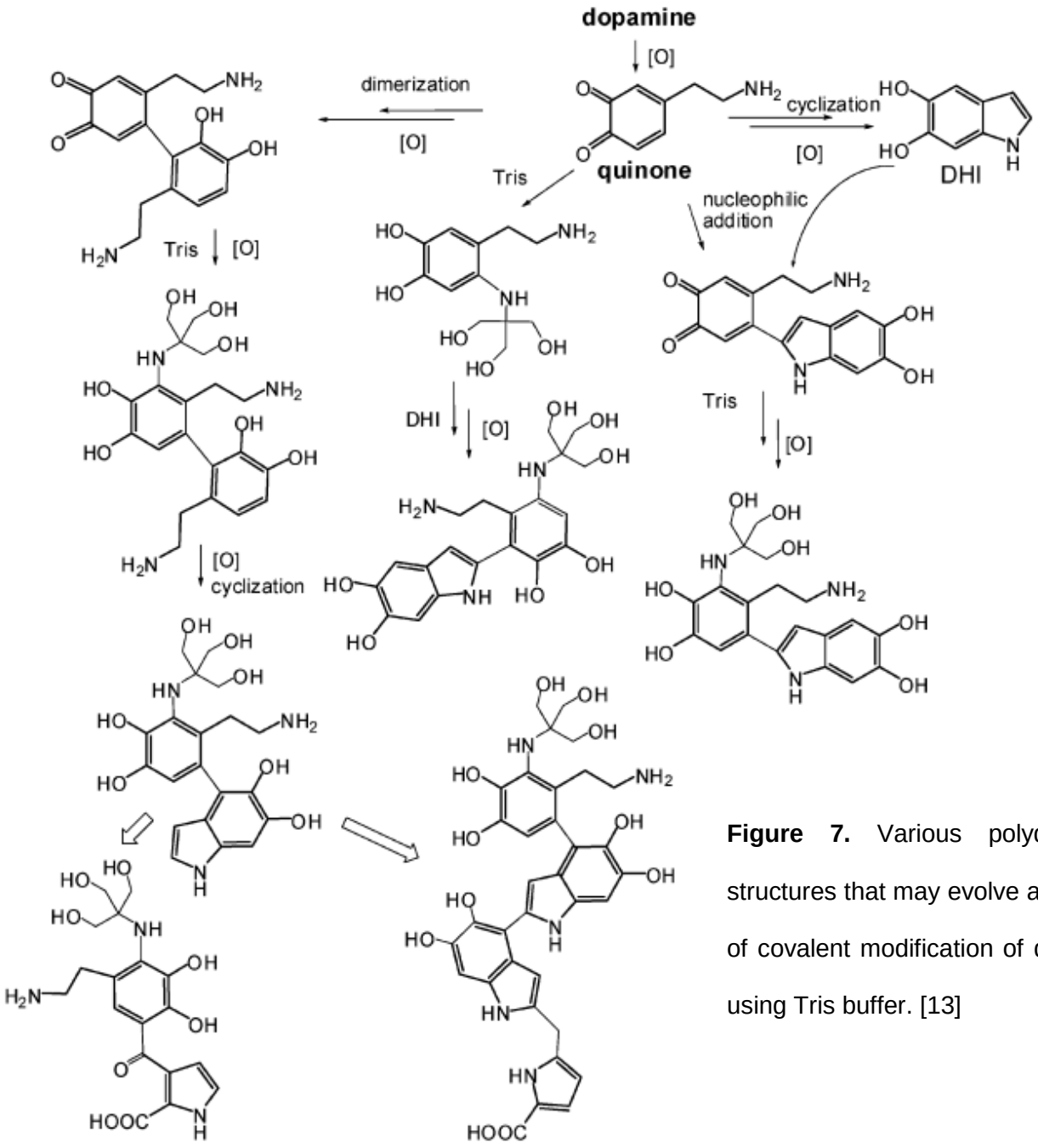

Figure 7. Various polydopamine structures that may evolve as a result of covalent modification of dopamine using Tris buffer. [13]

ammonia molar concentration considerations is not sufficient to inhibit PBS-mediated interactions. Ultimately, a PDA film made via oxidation in aqueous solution must be blocked from any potential to be polymerized to a higher degree when exposed to the PBS.

1.2.3 Polydopamine Thin Films and Coatings

To expand on why this research is novel, we again consider how PDA can be coated onto a surface. The deposition of polydopamine to a charged or metallic surface is an energetically favorable mechanism and can be done at STP by dip-coating into a pH-calibrated aqueous or buffered solution of dopamine and removing it after a few hours. [1] It can even be deposited via an electrolytic cell. [2] As the redox chemistry has been overviewed, it can be understood how this imparts a polydopamine thin-film coating on many types of substrates (including PTFE!) via strong bonding potential between its catechol and amine functional groups and π-π / H-bonding / cation-π mechanics. [6]

The research associated with the film deposition will be discussed in a later section. In the oxidation of dopamine, this dip-coat film deposits readily and varies in thickness depending on the length of time the substrate remains submerged or dopamine concentration/other reasons). [1] It was discovered experimentally that this is more difficult to do with ceramic microcrystals with no ligands for dopamine to react with.

This does not mean that the coating of the ceramic crystals does not occur- only that it is not uniform and possibly not favorable. Additionally, the fluid dynamics of a fluid in vortex are perilous for the health of fragile ceramic crystals- leading to some particles with excessive coatings, some particles with partial coatings or dotted with PDA nanoparticles, and many fragmented materials- some with only a vague spotting of polydopamine.

1.2.4 Advancing Degrees of Polymerization of Polydopamine Materials

As an example, take a YLF crystal that has somehow been completely coated with a visible polydopamine film (notable in bright/dark field microscopy and SEM) of polydopamine deposited via aqueous oxidation. The final goal is to conjugate an enzyme to this surface. Knowing that enzymes denature when not in buffered solution, PBS is utilized. However, dopamine can be polymerized by buffered solutions. Intuitively, the issue presents itself: What happens to the surface film coating when exposed to the PBS which has its own mechanism of reaction with DA/PDA? The original system also called for the usage of glutaraldehyde (GA) and gives us the same query: What is the reaction between GA and DA/PDA?

1.2.5 Dopamine-Glutaraldehyde Reactivity

In this model, an enzyme is conjugated to a glutaraldehyde (GA) molecule (**Figure 8**) bound to a polydopamine surface deposited on a YLF crystal. This creates a covalent linking system at the amino acid residues that GA interfaces with, similar to other surface conjugation methods [15]. When exposed to dopamine, however, glutaraldehyde has a fascinating crosslinking effect due to its high affinity for primary amines.

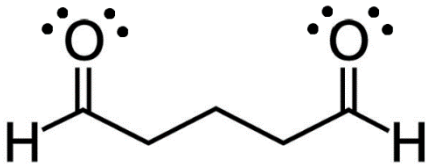

Figure 8. Structure of glutaraldehyde (GA), (Wikipedia)

The polymerization reaction between DA-GA (called PDAG here) is interesting because it produces macroscopic films in solution with no intentional substrates (i.e. only the glass of the vial and the PTFE of the stir bar are possible deposition sites). It is fascinating because these films no longer possess identical optical properties as polydopamine synthesized through oxidation (also, perhaps, via buffered solutions but this is just speculation). Unfortunately, they also do not coat surfaces with the same ease. Because of this, the method by which this new PDAG coat was being spread over a surface was modified from standard temperature and

pressure to be hydrothermal. These methods and procedures will be discussed later in the text body. It was experimentally determined that PBS did not have a noticeable effect on PDAG films.

1.3 Motivation

To summarize the system thus far, it is a ceramic crystal of one of two types and geometries- rhombohedral YLF prisms or hexagonal β-NaYF discs/plates and this is coated with a PDA film with complex surface chemistry. Only one chemical mechanism is actually used but many mechanisms had to be picked apart and through to find the viable path to achieve the target goal. Part of the motivation behind this work came principally because it has been previously observed that when ceramic crystals such as these come into contact with each other in the confines of an optical trap, they engage in a dynamic process known as OA or “oriented attachment” wherein the crystalline planes align themselves and the crystals fuse together. This is a very interesting process but is not helpful when trying to study single crystals. This leads us to a question behind the motivation: Can the surface be modified to disallow OA while not interfering with the optical properties of the crystal?

For a surface that is negatively charged with only OH^- available for conjugation, the number of reactions available for enzyme conjugation are severely limited. How can we expand our library? For trapping objects in an optical trap for study, the permanent aggregation of materials is undesirable. How can we make objects not stick together?

The engineering of a polydopamine coating and film was the initial aim of this project but it evolved quickly into polymer crosslinking as my education in the optics bay deepened- native polydopamine would never work for our purposes because of its light absorption profile (it’s black). Through literature, it was found that polydopamine materials can optically heat with a tremendous temperature profile. [16]

2. Body of Text – PDA vs. PDAG

2.1 Methods

2.1.1 Reagents

Dopamine HCl (DA, Sigma Aldrich, 98%)

Ammonium Hydroxide (28-30% NH_4OH, J.T. Baker)

Glutaraldehyde (50:50, GA:H_2O, Fisher Scientific)

Sodium Fluoride (NaF, 99%, Fisher Scientific)

Yttrium Nitrate ($Y(NO_3)_3 \cdot 6H_2O$, 99.8%, Sigma Aldrich)

Ytterbium Nitrate ($Yb(NO_3)_3 \cdot 5H_2O$, 99.9%, Sigma Aldrich)

Lithium Fluoride (LiF, 99.99%, Sigma Aldrich)

Ammonium Bifluoride (NH_4HF_2, Sigma Aldrich)

Phosphate-Buffered Saline (PBS, Sigma Aldrich, Biotech Certified)

MilliQ Water (diH_2O, ThermoScientific, GenPure UV/UF xCAD)

Ethanol (EtOH, UW Chemistry Stockroom)

2.1.2 Methods Used

2.1.2.1 Standard Synthesis of PDANP – Monodispersed nanoparticles and Film Coats

In the standard synthesis of PDA monodisperse nanoparticles (PDANP), a stock solution of 50mg/mL Dopamine hydrochloride in water is first prepared. A pipette is used to mix 100uL (corresponding to 5mg) into 9.75mL ethanol + water (2mL + 7.75mL, respectively) solution held at 30°C being stirred by a 1/4” magnetic stirrer at 400rpm in a 20mL borosilicate glass scintillation vial. Time zero is taken upon the addition of 0.150mL ammonia and the final time point is taken at 24h. Particles of uniform size and monodisperse nature result with an average particle size of ~300nm and a PDI of less than 0.05. After an excessive period of time in the reaction bath, the particles degrade into coatings on the interior of the borosilicate vial and also on the PTFE-coated stir bar. Adjustments of any of these values results in an alteration of particle size and/or monodispersity.

The particles are purified via centrifugation (5min @ 6000rpm) twice. First with ethanol in a 50mL falcon tube, then transfer to a 15mL falcon tube for a second ethanol wash, followed by MilliQ H_2O twice, sonicating briefly in between washes.

2.1.2.2 Synthesis of PDA using Copper Catalysis -

In the synthesis of PDA amorphous materials using copper (sourced from copper sulfate), the procedure of the standard synthesis of PDANP is modified to use 0.150mL of $CuSO_4$ [30mM] instead of ammonia. Time zero is taken upon the addition of copper. This reaction was halted and purified after 22h.

2.1.2.3 Stirring YLF crystals in PDANP

This procedure took previously-synthesized YLF crystals and stirred them at 400rpm with previously-prepared PDANP. Direct results are shown throughout **Section 2.2**.

2.1.2.4 Film Formation over YLF Surface & Enzyme Conjugation

This takes previously synthesized YLF crystals and stirs them in the reaction volume from the Standard Synthesis of PDANP.

2.1.2.4.1 Multiple Rounds of Stirring YLF Crystals in PDA Solution

This takes the product from 2.1.2.4, purifies it, and injects a fresh volume of dopamine solution. This is done in sequential rounds (up to 3 were performed, once every two hours)

.

2.1.2.4.2 Stirring PDA@YLF in Glutaraldehyde + PBS

Purify the product from the previous section and stir it in a 1.25% solution of Glutaraldehyde in PBS for (30 minutes).

2.1.2.4.3 Stirring Glu@PDA@YLF in PBS to Conjugate Target Enzyme

Centrifuge to purify the product from the previous section using PBS instead of H_2O and add it into 50mL PBS containing the target enzyme. Allow this to stir slowly at 4°C for 96h. Purify by centrifugation in PBS and store at 4°C.

2.1.2.5 PDA Synthesis via Glutaraldehyde (GA, 50:50) Percent Volume

The standard PDANP synthesis is modified to remove the ethanol and ammonia contents. Glutaraldehyde volume percentages were prepared in water. Six 20mL scintillate vials containing a final volume of 10mL GA (50:50) + H_2O are prepared with the following volume percentages: 0.0005%, 0.005%, 0.05%, 0.5%, 1.25%, 2.5% Volume percentages lower than 0.5% were prepared via serial dilution. Time zero is taken at the addition of the dopamine source. The reaction is terminated at 120 hours.

2.1.2.6 Dynamic Light Scattering and Zeta Potential

DLS and Zeta Potential scans are taken to measure the particle size (based on the average particle size, Z-avg), monodispersity of the system (based on the polydispersity index- PDI- of the suspension, lower is more monodisperse). Samples are prepared by taking 10uL particle suspension and diluting in 990uL diH_2O. After mixing, 100uL of this is added to a Malvern Zetasizer disposable cuvette and mixed using 900uL diH_2O. After the DLS measurement is completed, the sample is removed using a cuvette and injected into the zeta potential-reading cuvettes.

2.1.2.7 Hydrothermal synthesis of YLF crystals with PDA as a surfactant

0.210g of LiF combined with 0.680g NH_4HF_2 and dissolved in 7mL H_2O. Yttrium and ytterbium nitrates, 1.74g $Y(NO_3)_3$ and 1.12g $Yb(NO_3)_3$ are dissolved in 7.20mL and 0.8mL, respectively, and combined with this. Dopamine mass of 0.310g is dissolved in the solution as final volume is brought to 15.0mL with H_2O. Measured pH is ~7.0. Reaction temperature is 220°C for 72h.

2.1.2.8 *Hydrothermal synthesis of PDA*

Standard synthesis of PDA in a Teflon liner at 220°C for 72h

2.1.2.9 Hydrothermal Synthesis of PDAG nanoparticles

Standard synthesis of PDA with an additional 0.100mL in a Teflon liner at 220°C for 72h

2.1.2.10 Hydrothermal synthesis of PDA and PDAG nanofilms on previously-synthesized β-NaYF

Methods from 2.1.2.8 or 2.1.2.9 plus ~50mg β-NaYF (previously synthesized)

2.1.2.11 Enzyme Conjugation to PDAG-coated β-NaYF

Product from 2.1.2.10 is purified and gently mixed in PBS at 4°C with target enzyme for surface conjugation for 96h.

2.1.3 Equipment Used

Apreo Variable Pressure SEM, ThermoFisher Scientific

Nikon Industrial Microscope ECLIPSE LV150/LV150A

1020nm Laser

Heratherm Heating and Drying Oven, Thermo Scientific

Parr PTFE hyrothermal synthesis liners (4600 & 4700)

PTFE Stir Bar

Hot/Stir plate

4°C Refrigerator

Mettler Toledo Analytical Balance Model# MS104TS/00

Ultrasonicator

Vortex Mixer (Fisher Scientific)

Centrifuge 5430 (Eppendorf)

Centrifuge 5418 (Eppendorf)

Malvern Zetasizer Nano Series

ThorCam

ThorLabs TED200C Thermoelectric Temperature Controller

ThorLabs LDC200C Laser Diode Controller

Piezo Stage

2.2 Results

2.2.1 PDANP Size Control Parameters

To open the door on PDANP synthesis, a parameter test series was put together, shown in **Table 1**. This test explored the effect of changing the mass of dopamine, the molar concentration of ammonia, and the temperature of the reaction volume.

	Solution 1		Solution 2		Ammonia		24h time point		
Trial #	H2O (mL)	EtOH (mL)	H2O (mL)	DA (g)	NH4OH (mL)	Temperature (°C)	Avg Particle Size (d.nm)	PDI	Zeta (mV)
1A	4.50	2.00	0.500	0.0500	0.150	20	1483.33	0.533	-15.5
1B	4.50	2.00	0.500	0.0250	0.150	20	625.1	0.0330	-25.3
1C	4.50	2.00	0.500	0.100	0.150	20	2262.3	0.172	+15.5
2A	4.50	2.00	0.500	0.0250	0.300	20	404	0.0530	-34.6
2B	4.50	2.00	0.500	0.0250	0.150	20	538.5	0.0160	-39.6
2C	4.50	2.00	0.500	0.0250	0.450	20	481.6	0.0530	-43.5
3A	4.50	2.00	0.500	0.0250	0.150	4	953.2	0.239	+10.0
3B	4.50	2.00	0.500	0.0250	0.150	20	N/A	N/A	N/A
3C	4.50	2.00	0.500	0.0250	0.150	35	602.4	0.0120	-49.8

Table 1. Size and character control analysis using DLS. Adjustments are shown to have a direct impact on size and, seemingly, zeta-potential. For brevity, samples with PDI < 0.05 are regarded as equivalently monodisperse species. Sample 3B was not recorded due to redundancy.

With the results obtained, it was shown that significantly lowering the dopamine mass (or having much lower dopamine to ammonia ratio) produces a broad dispersion of particles. Having high DA:NH_4OH yields very large particles that are more monodisperse. These particles have a reasonable variation in their zeta potential. Inversely, when the mass of dopamine is unchanged but the ratio of DA:NH_4OH is again made large, the particle size is seen to decrease alongside a maintenance of the polydispersity (~0.530). When the temperature is lowered, PDANP forms

larger, less monodisperse systems. As the temperature is raised, the system formed is extremely monodisperse. The takeaway from this is that temperature is a significant driving factor for uniformity in polydopamine systems.

2.2.2 Coating of YLF Crystals

Initially, YLF was simply spun in solution with PDANP to see what kind of interaction there was (if any). The results of this are shown in **Figure 9**. It can be seen to appear as somewhat of a massacre as there is no charge-repulsion between YLF crystals. This results in brittle, ceramic crystals slamming into each other and shattering because of the force of impact at high rotation. Further damage is accrued during vortexing steps throughout purification. Gentle inversion and sonication are used to mix and clean the product.

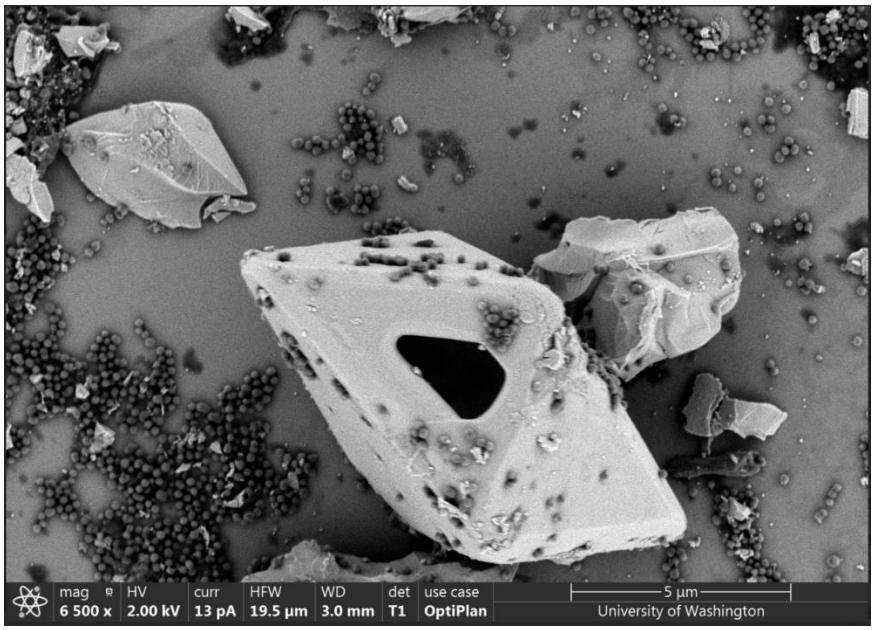

Figure 9. Fragmented remains of spinning YLF crystals with PDANP. Very few adhesion interactions with the surface can be seen. The dark species are PDANP. Photo credit: Lars Forberger

It is important to note in this figure that these nanoparticles are the result of preparing PDANP via oxidative synthesis. When this coating is observed over any surface, it is taken to have the same physicochemical characteristics.

After many attempts to coat YLF crystals, uniform PDA film coats were finally grown after three successive (and lengthy) rounds of coating and purifying the same particles. The step-wise growth of this is shown **Figure 10**. All of these samples were taken from different dispersion levels of

the purified particles. YLF crystals with greater levels of coating would fall out of solution and form a blackened layer at the bottom of the vial, YLF crystals with slight to moderate coatings would be suspended above them, and above the moderate coatings were YLF crystals with little to no coatings.

The step-wise mechanic appears to begin with a scattering of PDANP finding a rare region to adhere to, seen in **Figure 10a**. The addition of 5mg of dopamine monomer begins to seed the surface species seen in **Figure 10b, c**. Further addition of dopamine monomers grows these surface-adhered films distinctively and uniformly across the ceramic surface (even into crevices and carved out hollows) and also produces a new polydopamine species which can be seen on the surface of the particle in **Figure 10d** in the close-ups of **Figure 10e, f**.

If this polydopamine species were the same as the film, it would charge similarly and have more uniformity to it. As has been thoroughly discussed by this point, the production of polydopamine products is very direct so why were monodisperse PDANP not formed at the surface? Based on polymer chemistry concepts [17], the answer appears to be that the capacity of dopamine monomers and their downstream oligomers to oxidize with themselves and each other created the desirable conditions for a polydopamine species to form that does not charge in the same way as its other nanoparticles and film.

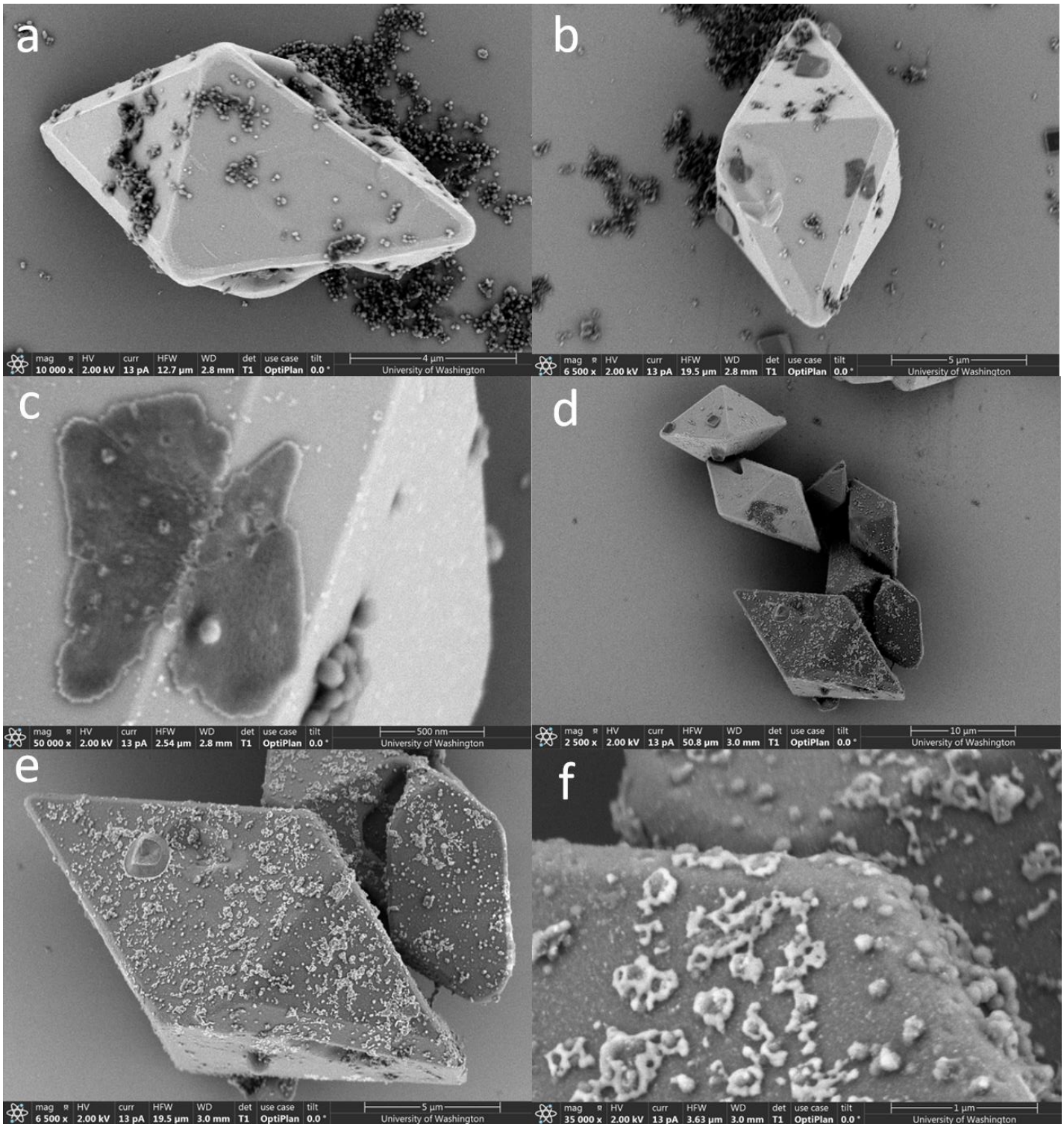

Figure 10. Successive coatings of PDA over YLF crystals obtained by taking aliquots from three separated layers in the purified fluid. The stepwise mechanism can be seen following a), c), and e) as PDA oxidative film growth proceeds over the ceramic surface. Photo credit: Lars Forberger

2.2.3 Enzyme Conjugation to PDA Film Surface in PBS

Because discoveries can be made both systematically and through inventive error, a small mass was immediately moved into the downstream step of mixing with 1.25% GA in PBS, purified via centrifugation, and then stirred at 4°C in PBS with the target enzyme to conjugate for 96h. The final results of these efforts are shown in **Figure 11**.

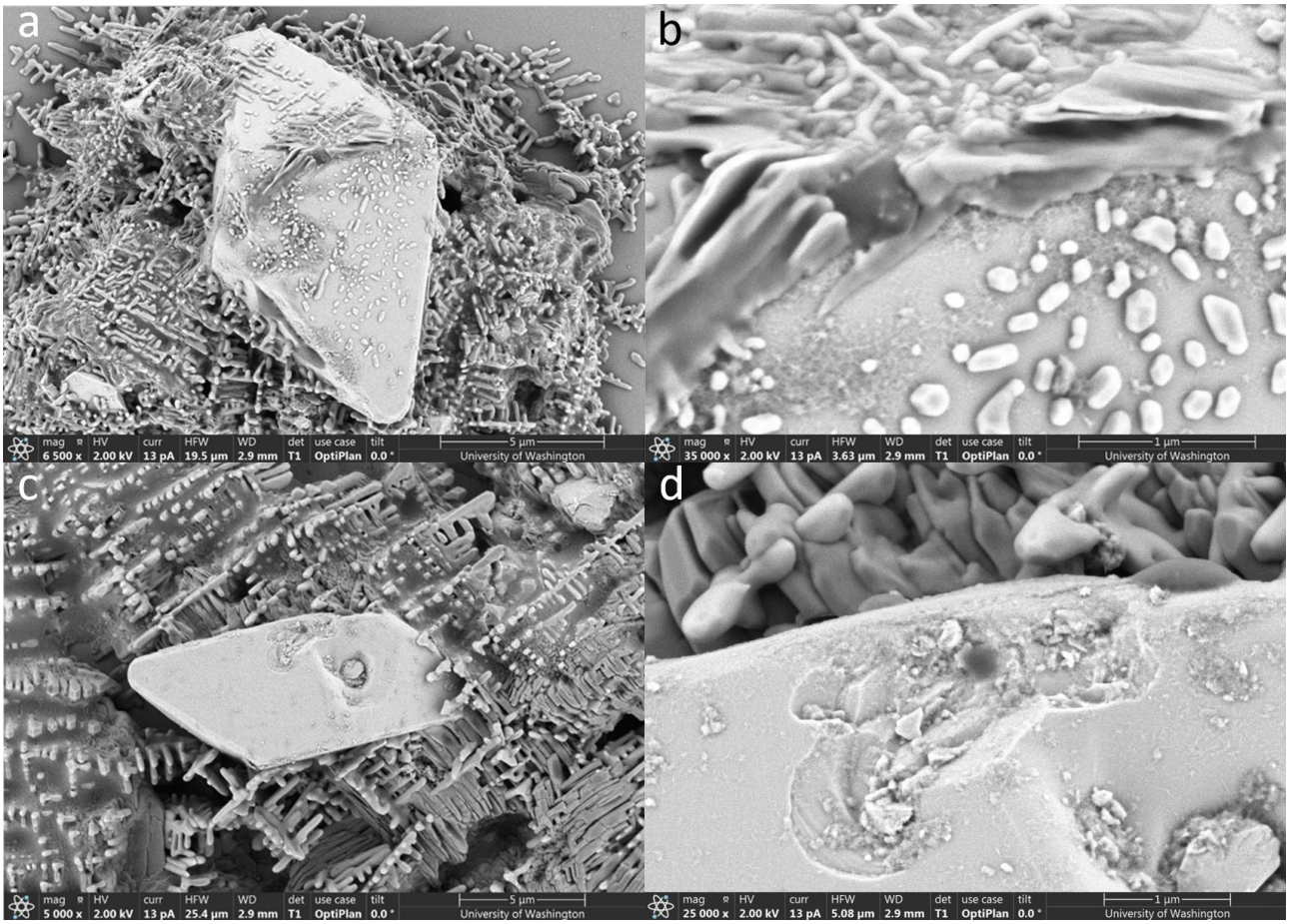

Figure 11. Results of attempt to conjugate target enzyme to the polydopamine film surface spread over YLF crystals. Film morphology is shown to have completely disappeared, leaving the crystal surface bare with a polymeric “slag” around it. The polymer aggregate is not completely detached in all cases, as can be seen in a) and b) where the polymer film still has sites of deposition on the YLF crystal. Photo credit: Lars Forberger

This would appear to be a significant failure. Fortunately, the chemistry of dopamine and its oxidative monomers/oligomers is known and it guides the understanding to what, exactly, is being shown in these SEM images. A new question arises: What are the differences in reaction and/or product species when dopamine is exposed to PBS and glutaraldehyde separately?

2.2.3.1 The Differences in Product Species of PDA-PBS and PDA-GA

Although the reduction of Cu^{2+} by dopamine was additionally studied in this particular subsection, only the results of PDA-PBS and PDA-GA reactions are discussed in this body. To begin, knowing that GA reacts strongly with primary amines such as those of dopamine monomers, if glutaraldehyde is able to bridge any DA monomer species together, it must similarly bridge any downstream oligomeric species that also contain a primary amine(s). The question that needed to be answered was: what is the product formed if given unlimited time and without intentionally altering the solution pH using ammonia? The experiment outlined in **Table 2** shows the product of mixing (400rpm) 5mg of dopamine-HCl with serially diluted volume percentages of glutaraldehyde over the course of 120 hours at 30°C. The results of this experiment are shown in the images in **Figure 12**.

5mg dopamine HCl (50mg/mL stock solution), T = 30°C, t = 120h			
Sample ID GA (v/v)	**H2O (mL)**	**GA:H_2O(50:50, mL)**	**DA-HCl (50mg/mL)**
10%	0.900	0.100	N/A
2.50%	9.50	0.50	0.100
1.25%	9.75	0.25	0.100
0.50%	9.90	0.10	0.100
0.05%	9.99	0.01	0.100
0.005%	9.90	0.1 (10%)	0.100
0.0005%	9.99	0.01 (10%)	0.100

Table 2. Set-up to explore the possible product formed from the reaction between glutaraldehyde (50:50) and dopamine-HCl. The bottom two samples are prepared from the serial dilution of “10%” sample ID. Samples mixed continuously at 400rpm. V_F = 10.1mL

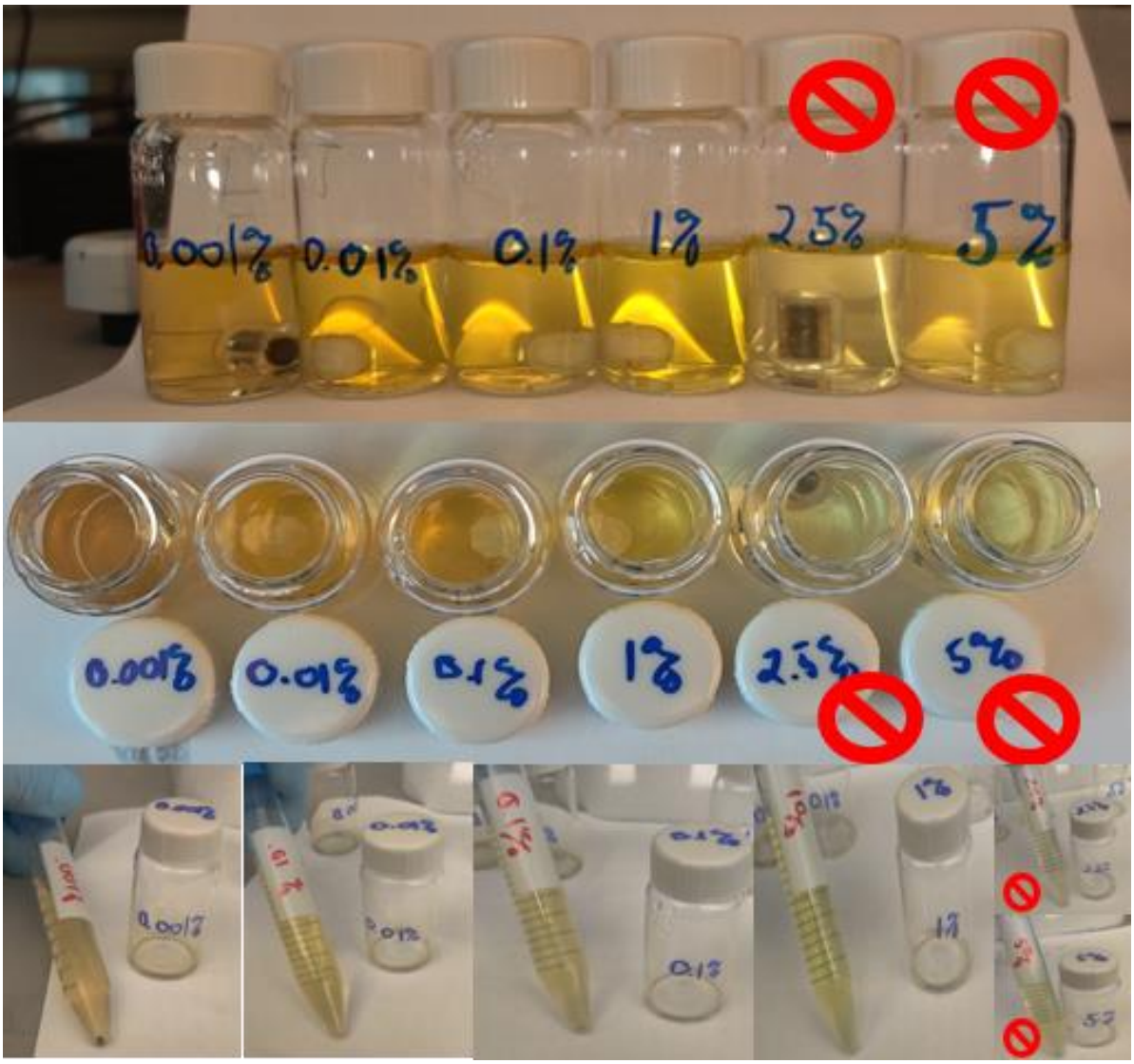

Figure 12. Samples set up to explore the interactions between DA and GA. The method of preparation (and true concentrations) can be found in **Table 2**. The discrepancy in the labeling is because the glutaraldehyde being 50:50 with water was not known at the time of preparation. This is corrected for the rest of the text and figures. Only samples “2.5%” and “5%” (corresponding to “1.25% and 2.5% from **Table 2**) did not produce a macroscopically visible product after centrifugation. Though it is difficult to see, there is a slight yellow film on the outskirts of the scintillation vials (Samples “0.001%” and “0.01%”).

This reaction was considered to be terminated at the time of the first centrifugation and was washed several times with MilliQ H_2O. For samples whose 3-times-centrifuged-and-washed-with-H_2O, macroscopic product were simple to prepare on glass slides, microscopic images were taken, shown in **Figure 13.** This material is identified as PDAG throughout the text.

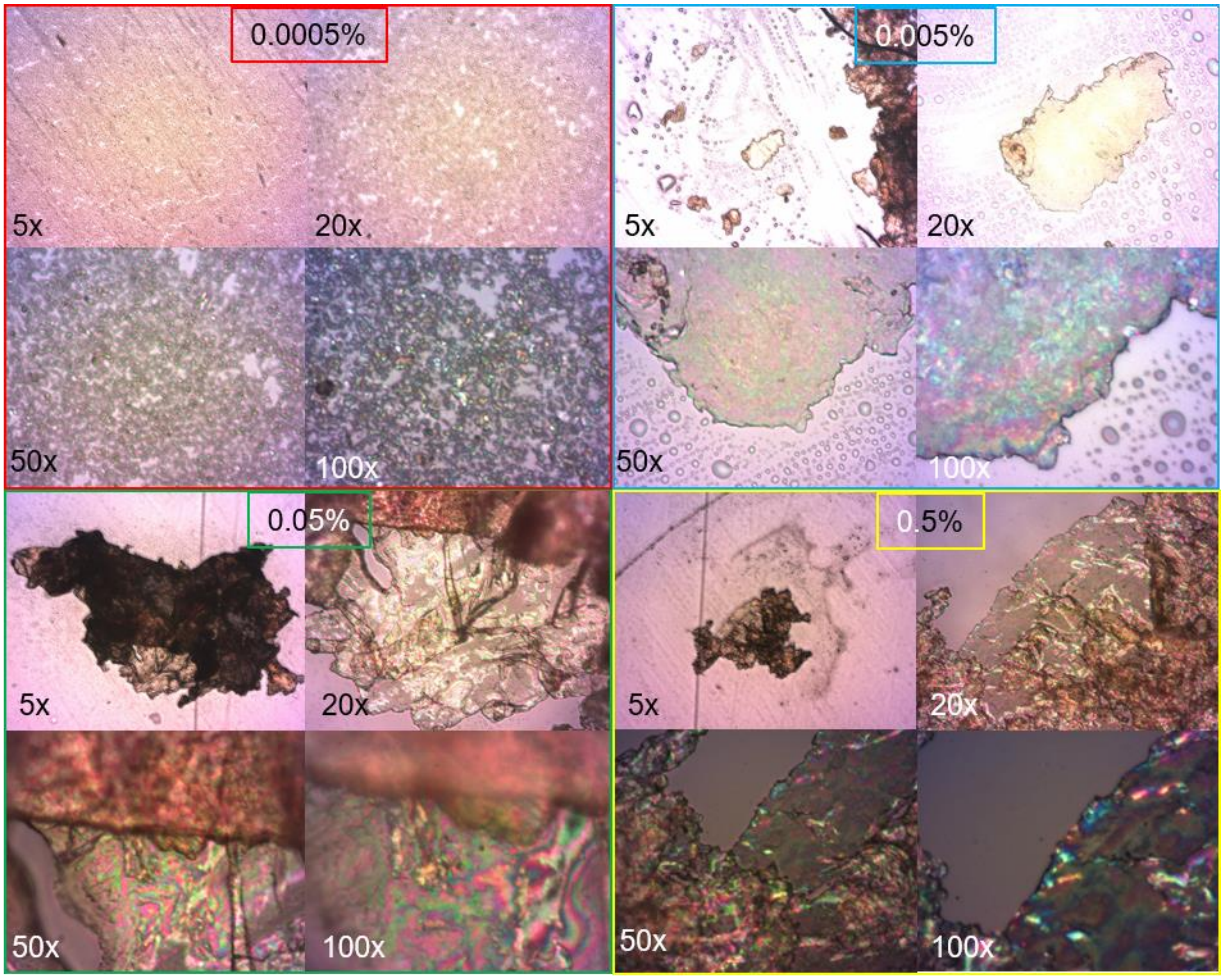

Figure 13. Microscopic images of PDAG products formed after 120h of stirring at 30°C and 400rpm. Film stability and thickness is observed to increase with increasing GA volume percent. The 50x and 100x images for Sample 0.5% were taken at a lower brightness to enhance the detail of the same polarization effect as can be seen in the lower volume percent samples.

In **Figure 14**, the film product of the “0.5%” PDAG sample was imaged. The film displays a remarkable flexibility in aqueous environment. It clumps to itself when removed and resumes its original shape when replaced.

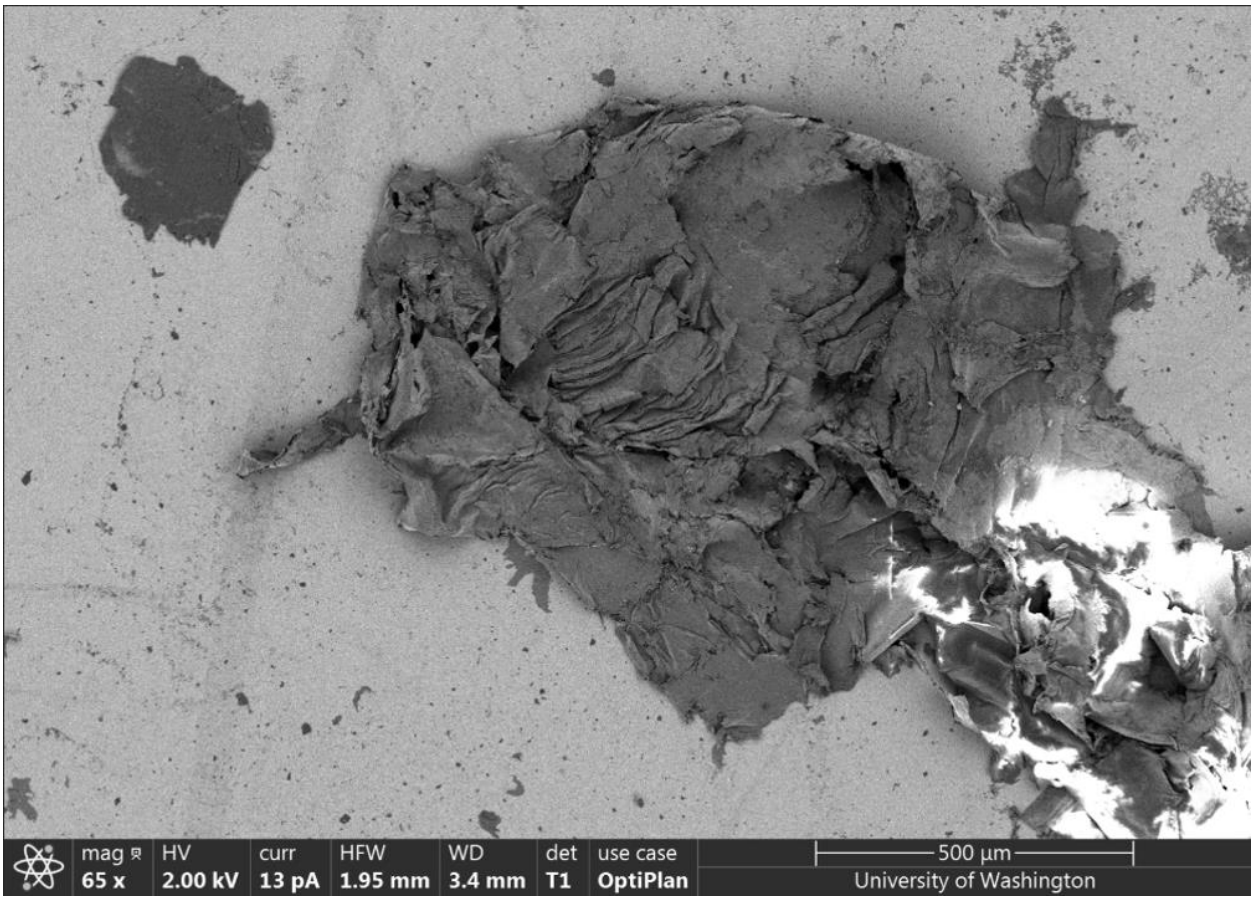

Figure 14. SEM image of the film formed from 0.5% GA and 5mg DA in solution. The reaction contents are the same as what would normally form monodisperse nanoparticles but, because of the presence of GA, films such as this form, instead.

Photo credit: Lars Forberger

The formation of PDAG was a surprise and spurred the development of a scattershot experiment, aimed to strictly qualify the extent other components of enzyme conjugation (PBS) participate. **Table 3** shows the reaction conditions and DLS results. **Figure 15** shows the synthesis vessels at time 0h and timepoint 19h. Microscopy images in **Figure 16** are taken at timepoint 72h.

5mg dopamine HCl (50mg/mL stock solution), 100uL of [32.6mM] DA-HCl, V_F = 10.0mL							
Sample ID	**H2O (mL)**	**PBS (mL)**	**YLiF4 (mg)**	**Glutaraldehyde (50:50) (mL)**	**% Glutaraldehyde**	**NH4OH (uL)**	**EtOH (mL)**
31-B	7.75	-	11.5	0.100	0.50%	-	2.00
31-C	7.65	-	12.1	0.100	0.50%	150	2.00
31-F	7.80	-	-	0.100	0.50%	150	2.00
31-G	-	7.80	-	0.100	0.50%	-	2.00

Table 3. Contents of the samples set up to explore the interactions between DA, GA, and PBS. The vials are paired to be controls for each other (one thing different between each). All vials contain 5mg of DA-HCl and the final volume of all samples is 10mL, 400rpm.

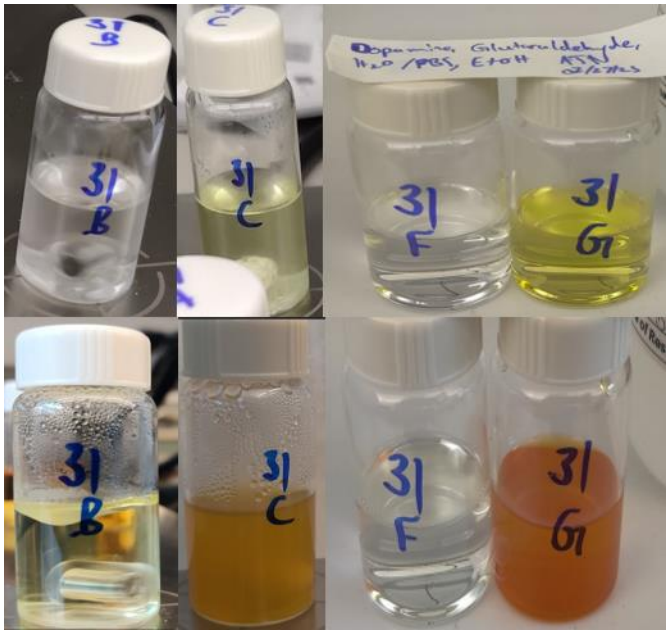

Figure 15. Samples set up to scattershot the interactions between DA, GA, and PBS. The contents of each can be found in **Table 3** above. The vials are paired to be controls. Top is the time zero, taken within 10min of adding DA. The bottom is after 19h. Sample 31-B shows expected reactivity and clarity whereas 31-C has become very cloudy, similarly to 31-G. It is important to note that 31-F and 31-G were never stirred at any time.

As a general reminder, although the concentration of $CuSO_4$ parameter was explored in this study, its results were not relatable. This is due to possible dispersion of Cu^{2+} ions throughout the PDA layer (which seems viable, based on experimental results).

In this scattershot study, the volume percentage of GA was chosen as 0.5% because the PDAG study showed the thickest, most macroscopically obvious film at this value. Additionally, when it comes to polymer crosslinking work, it is generally better to start with fewer crosslinking units and see what happens. Otherwise, the result is usually a gel which is undesirable for producing discretely coated particles.

	3x Centrifuged Product		Supernatant of Second Spin	
Sample ID	**Z-Avg (nm, avg)**	**PDI (avg)**	**Z-Avg (nm, avg)**	**PDI (avg)**
31-B	2136	0.941	890	0.740
31-C	310.2	0.024	262.7	0.068
31-F	476.4	0.260	302.1	0.633
31-G	6542	1.000	4272	1.000

Table 4. DLS data of the products purified via centrifugation and supernatant above the second spin fraction before being discarded. The supernatants were noted to contain measurable material. 31-F is highlighted because only pure synthesis fluid was analyzed for the first scan and only the first recovery volume fraction was analyzed for the “Supernatant of Second Spin” column. The sample was discarded after this because no further imaging or characterization could be done.

The DLS data obtained was difficult to use as a guide as sample 31-C was expected to have had a large Z-avg similar to 31-B due to the size of YLF crystals (2~8μm). The difference in this measurement is possibly because of a pipetting error where the sample was aliquotted from in the fluid volume or the particles failing to maintain suspension and settling out during the DLS measurement (possibly being discarded as outliers in early scans or being averaged out in the final

data report). It was still informative, however, as it indicated that there is highly monodisperse material present and able to be purified.

The most important sample to note in this particular experiment is sample 31-F due to its DLS results. Because this sample never produced anything in the way of a macroscopic product, only its pure synthesis fluid and second spin "supernatant" were analyzed (it wasn't even a supernatant- nothing could be recovered). Its reactive contents are DA, GA, and ammonia in an H_2O:EtOH solution so what sort of particles or materials could possibly be locally growing that would be so small and polydisperse? Some of the reaction products are shown in **Figure 16**.

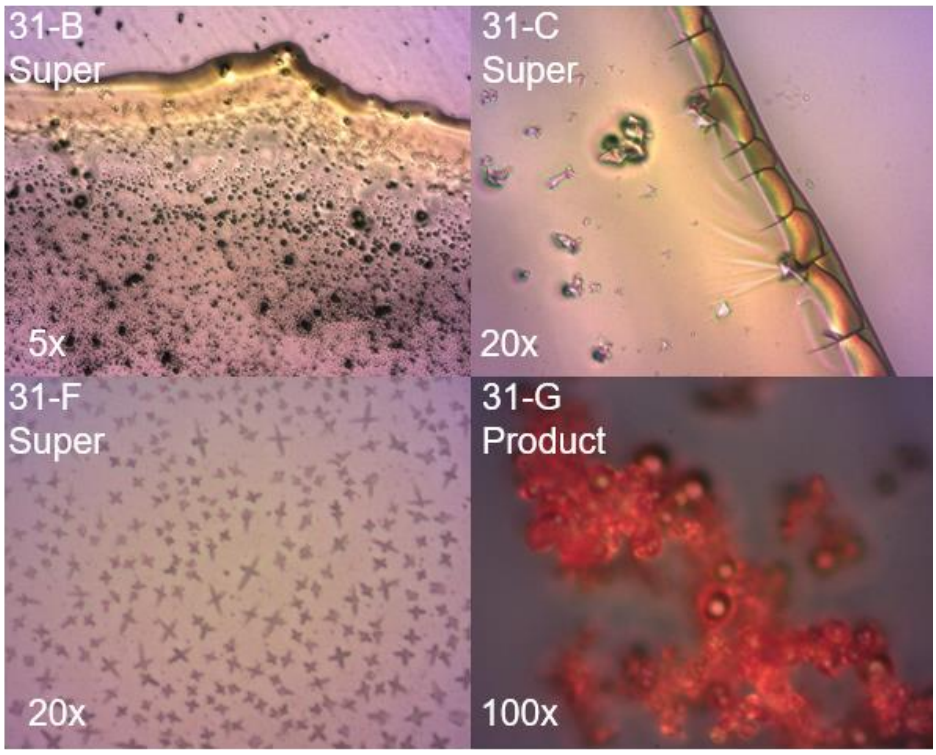

Figure 16. Microscopic images of products isolated from the supernatants (31-B, C, and F) and product (31-G) of samples in **Table 3** (after 72h). The formation of the same type of film between Sample 31-B and 31-C under the dynamic of a mixing fluid implies a greater interaction between GA and DA whereas sample 31-G, which contains PBS and GA and was stationary for the same timeframe, produced reddish particulates. The film in 31-C is cracked at the edges likely due to dehydration. When standing still, PDAG (31-F) seems to form as little X's or maybe wire-y growths.

Figure 16 mostly shows supernatant products. There are many images of the products and the information obtained from them does not go unnoticed. However, the fact of the matter is that there was strictly more downstream application information conveyed from these samples through the analysis of the supernatants than of the products (which became difficult to image with a microscope, besides). Because particles were able to be isolated from the supernatant, it was postulated that they must share something that keeps them level with their synthesis fluid. Under the microscope, some of these particles were observed to have lost a great deal of their birefringence- indicating interference (a coating, perhaps?). Sample 31-G in the above figure has its product displayed because it was a stationary deposition of amorphous aggregates that displayed some, albeit barely, spherical behavior.

Not completely analyzing the products would produce an incomplete narrative. An SEM image of Sample 31-C is shown in **Figure 17** below and, at the bottom (and slightly visible in the back) of this image, YLF crystals with coatings and nanoparticle decorations can be seen. The main foci are particles pointed to by the yellow(1) and magenta(2) arrows where two particles that possessed uniform coatings are believed to have been previously glued together (based on the material curvature, green arrow(3)) and, just above that, the bridge between the two particles (red arrow(4)).

This portion of the image is highly instructive because it shows that particles can be completely coated in PDAG and that there is a large excess of DA which, over the course of 72 hours, forms polydisperse PDANP (or possibly PDAGNP) that decorate the PDAG coat. This observation led to the question: considering that YLF takes 72h to form in a hydrothermal system that contains parts of both ammonia and water, is it possible to hydrothermally grow YLF crystals with dopamine as a surfactant?

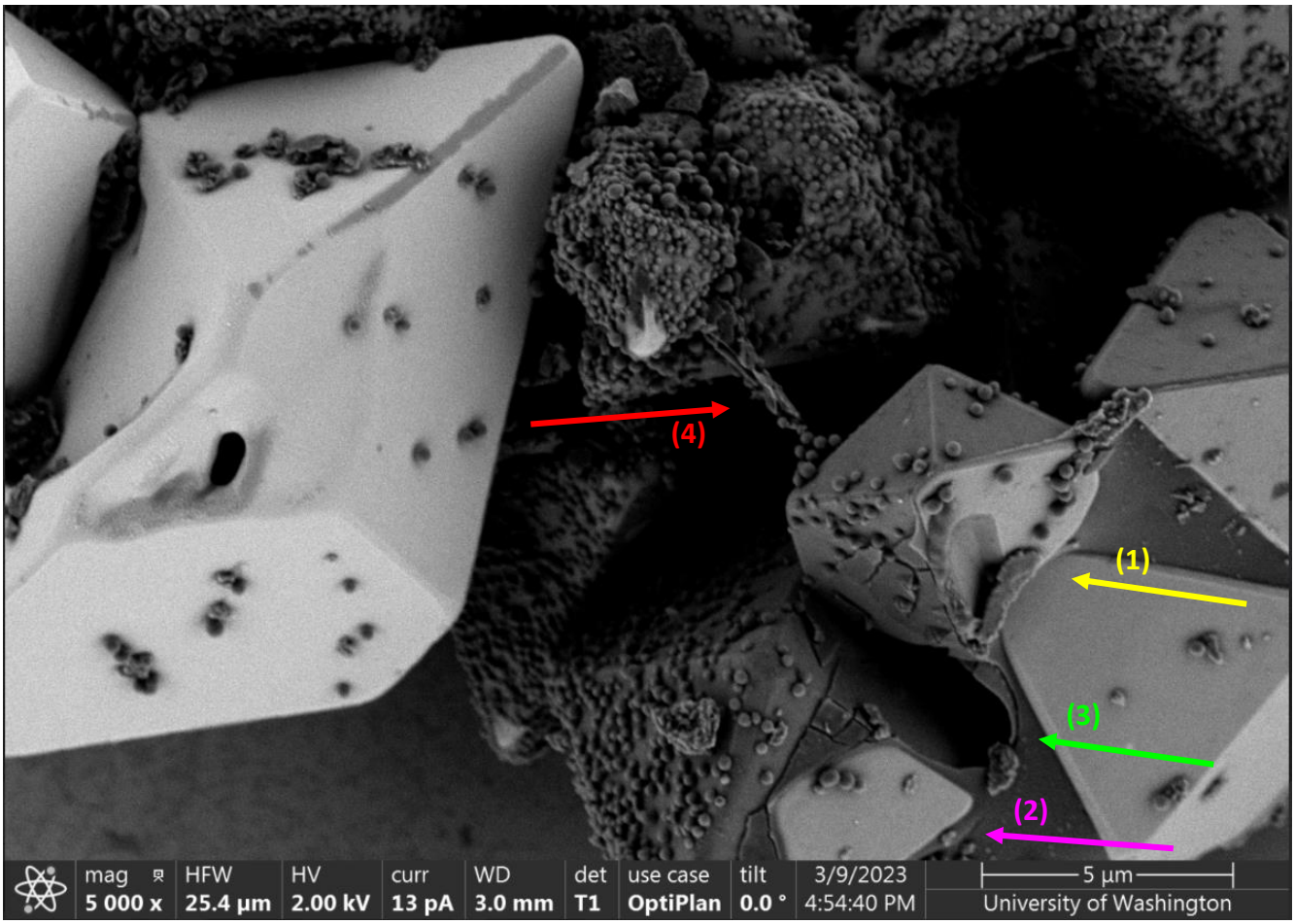

Figure 17. SEM image of Sample 31-C product. PDA coatings can be seen to have formed over YLF crystals at the bottom of the image but appear to have been split away from each other- these particles may have been stuck together and torn the PDA coating keeping them bound. In the back, YLF crystals appear to be completely coated and decorated with many PDA (or PDAG) nanoparticles while some YLF crystals appear to be mostly uncoated. Photo credit: Sankhya Hirani.

2.2.4 PDA + YLF Co-synthesis

A hydrothermal synthesis was put together to explore the capacity of PDA to deposit as a surfactant and create a uniform monolayer as a singular step. The synthesis parameters of lithium fluoride crystals were put together to study this. Yttrium and Ytterbium salts were not initially used in this particular experiment because Y/Yb insert themselves as dopants in the crystal structure of lithium fluoride ceramics and the objective geometry remains unchanged. This trial synthesis with 5-10mg DA was paused after 6h and a grayish solid product was purified- indicating formation of PDA materials, the full YLF synthesis was conducted for 72h at T=220°C with an additional 0.3702g DA-HCl and 0.150mL NH_4OH. From the understanding at this point, either the PDA layer would form based on the increase in ammonia concentration or something entirely different would happen because of the ionic strength of the solution. Shown in **Figures 18** and **19**, it is the latter case. Because the complete formation of PDA aggregates is more rapid (~30 hours) than the formation of crystalline ceramic crystals (~72 hours), the usage of dopamine as a stabilizing ligand in hydrothermal synthesis is not a reasonable pathway for the coating of a material. Thankfully, within the red circle at the very bottom

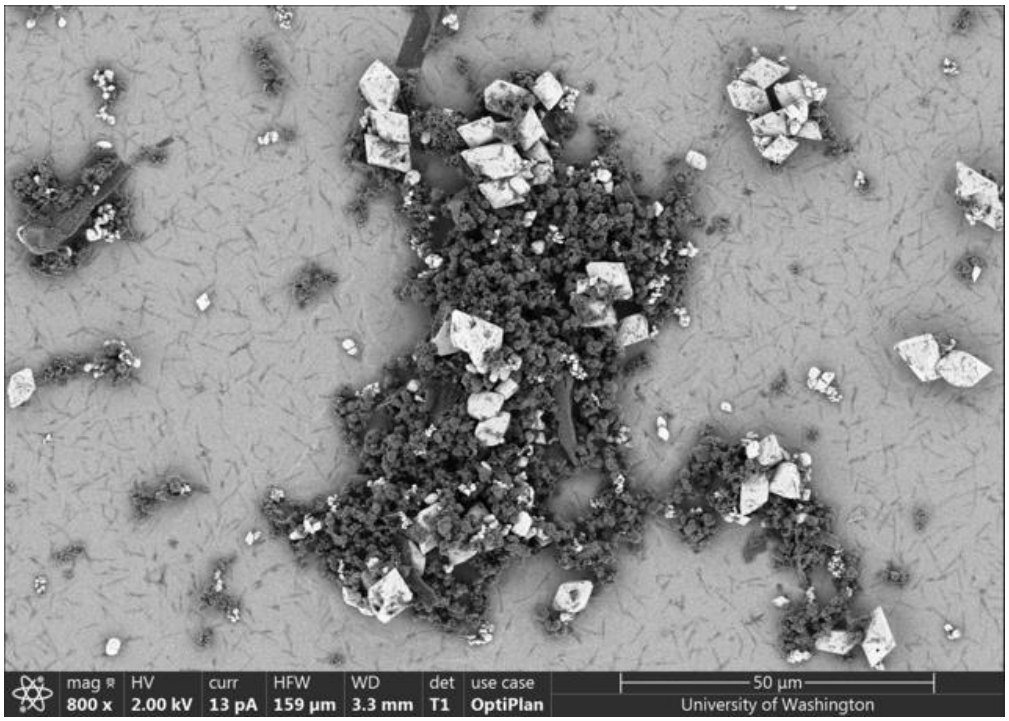

Figure 18. Purified products from attempting to use PDA as a ligand in the synthesis of YLF ceramic crystals. Mostly PDA aggregates form due to the complete growth of PDANP being much more rapid than that of YLF (~30h vs. ~72h). Many wire-like structures are noted to be present in the drop-cast sample region.
Photo credit: Lars Forberger

of **Figure 19** is another clue being sought after and is the topic of the next section. The new question being: what is the morphology of PDA that is hydrothermally synthesized?

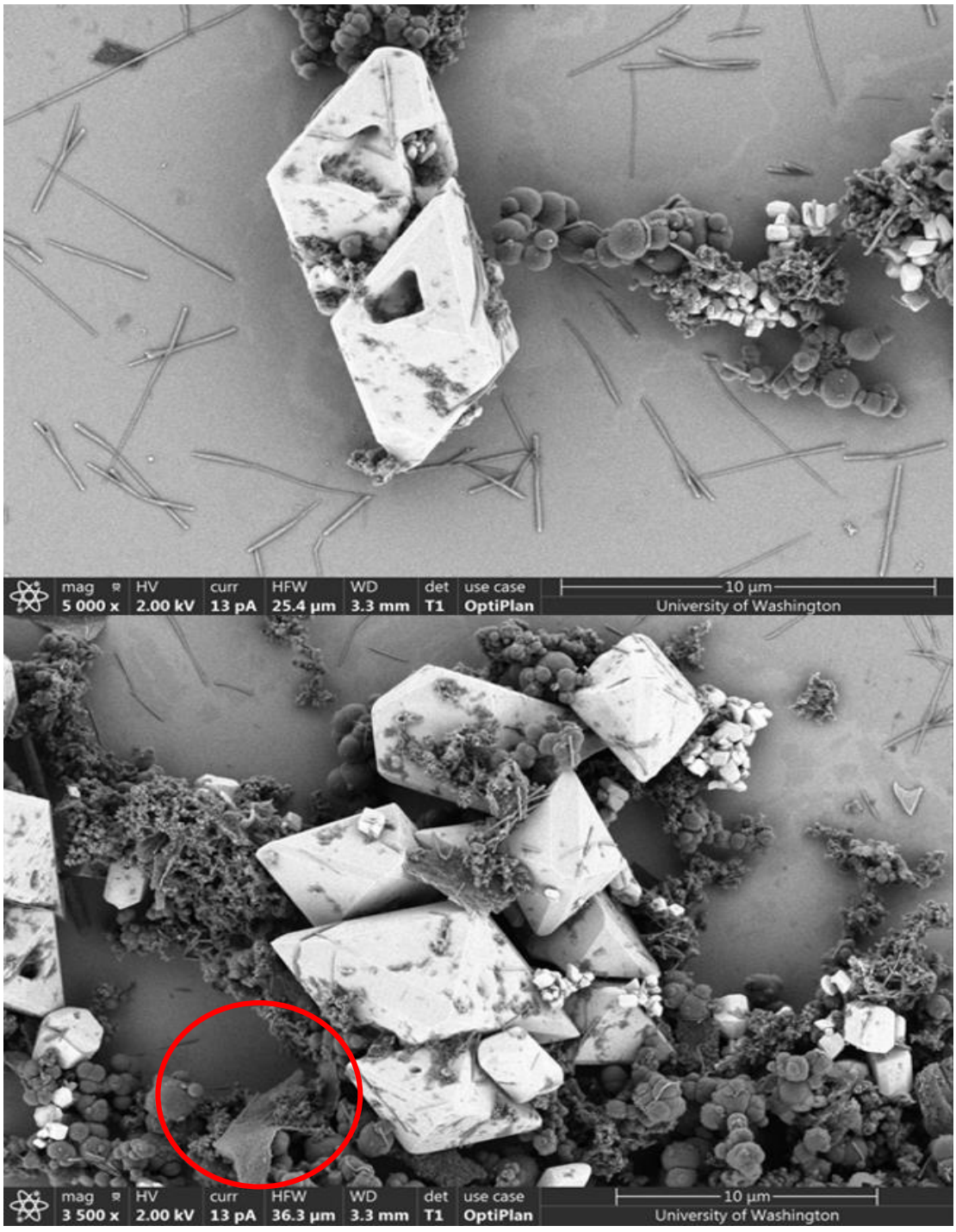

Figure 19. YLF synthesized in the presence of dopamine-HCl for 72 hours. Imperfect and mostly damaged YLF crystals form along with incomplete ceramic particulates. Polydopamine particles form and seem to sometimes smear over surfaces. Additionally, wire-like extensions are ubiquitously displayed around the entire sample- not just on the crystals.
In the bottom image, circled in red, is a polydopamine film formed in situ.
Photo credit: Lars Forberger

2.2.4.1 Possibly PDA Nanowires

Although it is not a direct focus of this project, it is important to point out the wire-like structures in **Figures 18 and 19** which are currently believed to have formed due to the ionic strength of the system. With their presence and the previous mention of coacervates, it is possible that they may be nanowires formed of polydopamine (otherwise, they could be foreign contamination). More research needs to be conducted to lend credence to this belief but, if it is not an unreasonable assumption, then the likely formation of these PDA nanowires should be due to the ionic strength of the hydrothermal synthesis fluid. An expanded view of the isolated material is shown in **Figure 20**.

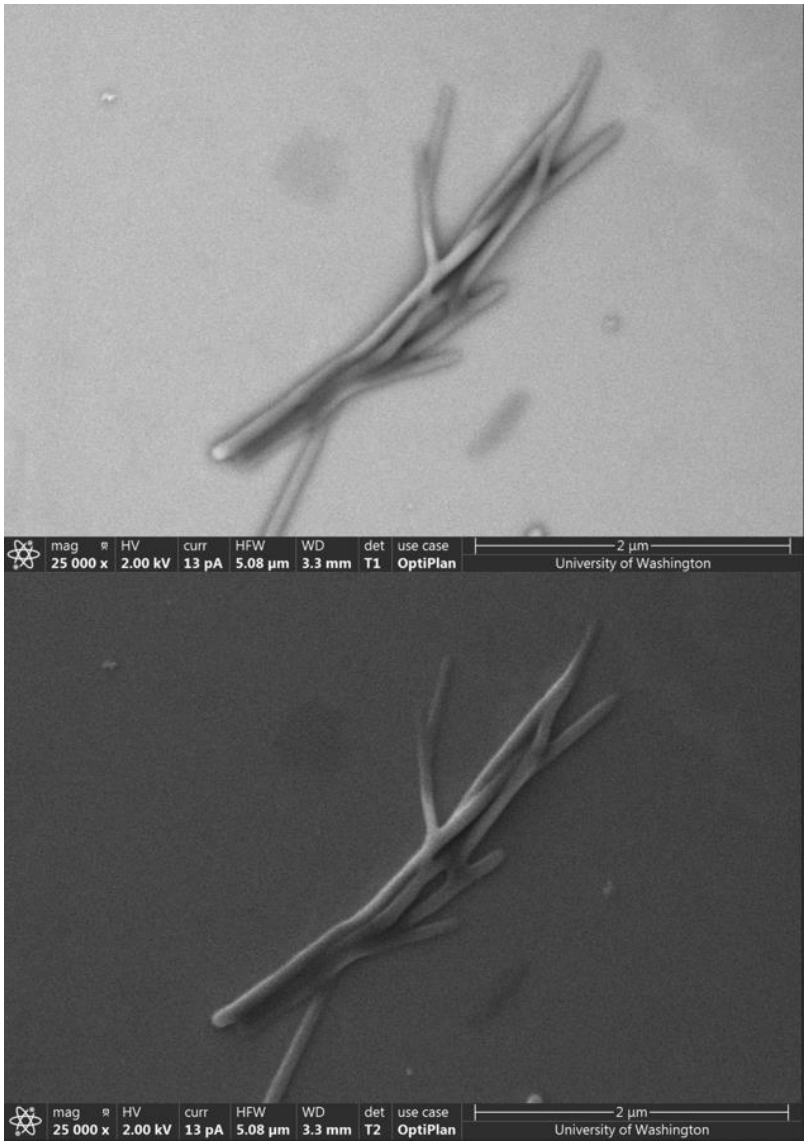

Figure 20. T1/T2 SEM images of materials purified from the hydrothermal synthesis of YLF with dopamine-HCl and ammonia added. Possibly hydrothermally synthesized PDA nanowires.

Photo credit: Lars Forberger

2.2.5 PDA and PDAG Hydrothermal Synthesis

From the contents of **Figure 18** and the contents in the red circle in **Figure 19**, it was observed that PDANP and PDA films both form within 72 hours at 220°C and hydrothermal pressure. It was important, then, to see what the morphology PDANP possess from hydrothermal synthesis. Additionally, since the formed product for the stationary PDAG microscopic little X's in **Figure 16**, it was curious to consider what sort of product they might also form from hydrothermally-agitated fluid. Shown in **Figure 21** is a side-by-side comparison of PDANP and PDAGNP (0.5% v/v) produced from T=220°C and t=72h. The side panels in this figure display expanded views of the nanoparticles produced from the hydrothermal PDAG synthesis. From this, it is conclusively shown that a product that differs significantly from the base synthesis forms under pressure. It is important to note that these PDAGNP are yellow whereas PDANP appear black. Despite this color difference being an expected outcome based on earlier study, it was still surprising to isolate yellowish solids. Another question arose: can this material, which forms a film at STP and forms a sphere at high temperature and pressure, encapsulate a crystal that has already been made and, if so, will the film be chemically robust against PBS, as it is predicted to be?

Unfortunately, the ration of YLF being pulled from was completely depleted. Fortunately, the Pauzauskie group possessed a surplus of β-NaYF hexagonal discs for testing. These discs have a ceramic surface that interacts with dopamine-based compounds in the same way that YLF does (note that $YLiF_4$ and β-$NaYF_4$ differ only by the underlined element which yields a different crystal structure but not a different surface reactivity for the purposes of this thesis). The use of these discs is also inclusive of exploring possible applications in other types of optical studies but this is outside the scope of this thesis.

Figure 21. SEM images of PDANP and PDAGNP (0.5% v/v) produced via hydrothermal methods at T=220°C and t=72h. PDANP (Top) has a fairly good size distribution and some amorphous blobs with a high surface roughness/porosity.

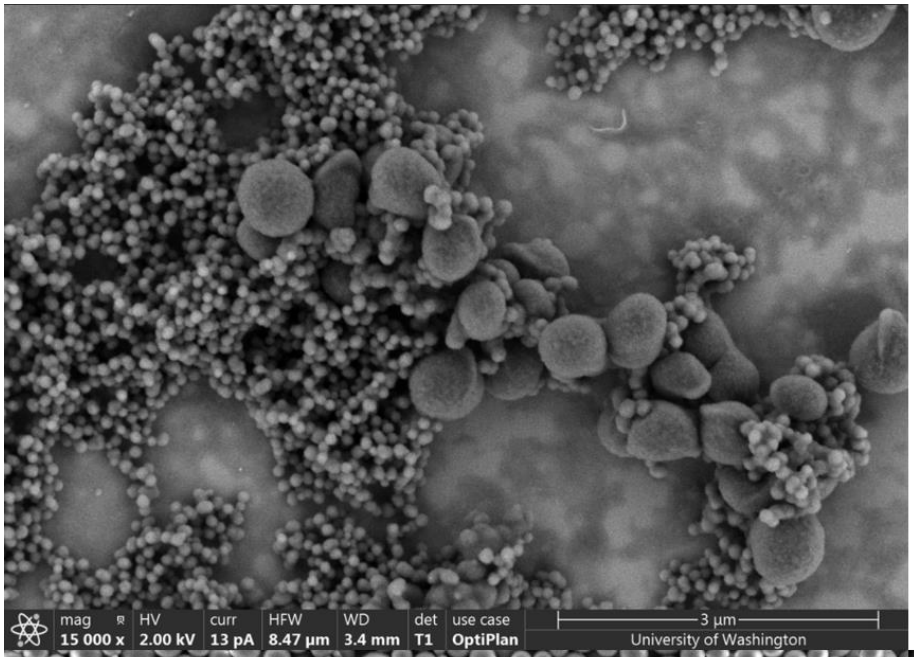

PDAGNP made with 0.5% v/v GA has a better native morphology control and appears to have a very low surface roughness. Right side panels are expanded views of PDAGNP.

Photo credit: Lars Forberger

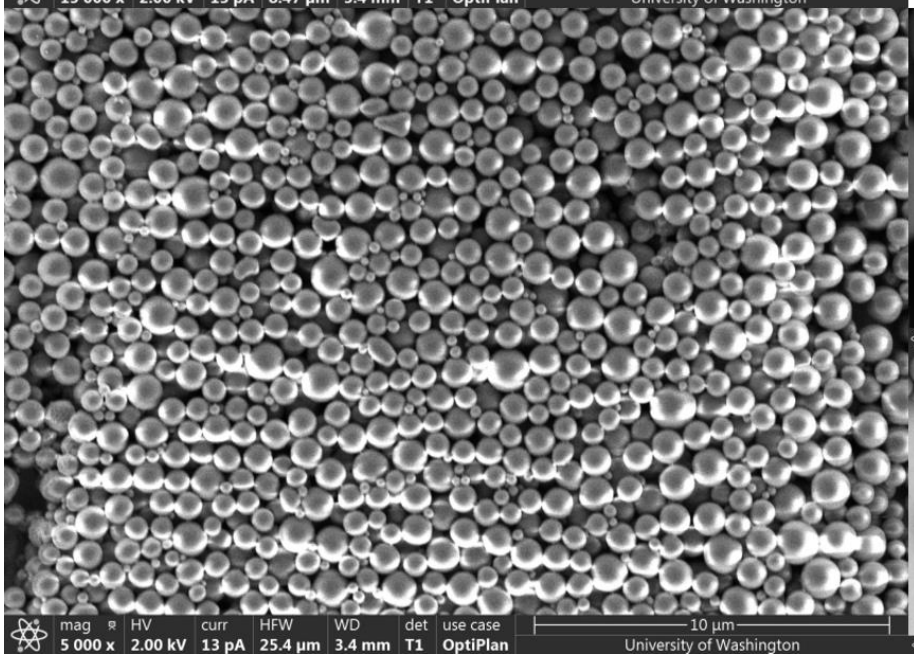

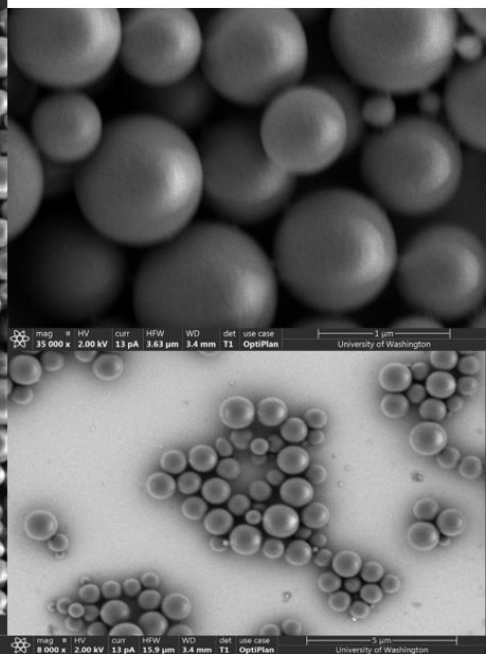

2.2.6 PDAG@β-NaYF Hydrothermal Synthesis

When YLF crystals are exposed to the NH_4OH:EtOH:H_2O mixture without dopamine, they are observed to dissolve. A sample of β-NaYF crystals was prepared in the same conditions and confirmed that it also dissolves without dopamine being present. On this basis, it is assumed that the surfaces of YLF and β-NaYF have similar enough reactivity to PDA and PDA film deposition to be regarded as the same.

After synthesizing β-NaYF, the hydrothermal reaction in **Table 5** was put together and allowed to react for 72h before being purified via centrifugation. Just as before, 0.5% GA (v/v%) was used and the products were slightly yellowish in color, as expected. **Figure 23** shows light microscopy and SEM images of beta-NaYF before and after PDAG coating. The difference between **Figure 23 (c, e)** and **(d, f)** is a coating of PDAG.

Reagent	**Volume (mL)**
50.5mg β-NaYF	
10mg Dopamine-HCl	
Glutaraldehyde (50:50)	0.10
Ethanol	2.00
diH_2O	7.65mL
NH_4OH	0.150mL
T=220°C	t = 72h

Table 5. Reaction conditions to coat β-NaYF with a thick layer of PDAG

In **Figure 24**, a more detailed view of a PDAG@ β-NaYF particle shows a high level of decoration- indicating either a large excess of dopamine in local fluid space during synthesis, or the concentration of glutaraldehyde is not enough to produce only a discrete phase of PDAG- meaning some PDA may also be getting produced. The level of coverage is still variable, as can be seen how in the bottom of **Figure 24**, the β-NaYF crystal has nearly the same level of coverage but not nearly as much decoration.

This now leads to the final experiment in the quest to design a ceramic-adhesive surface that produces a robust coating and also, hopefully, be used for enzyme conjugation. The last question to answer is: Will this PDAG coating maintain its stability when exposed to PBS and conjugate a target enzyme?

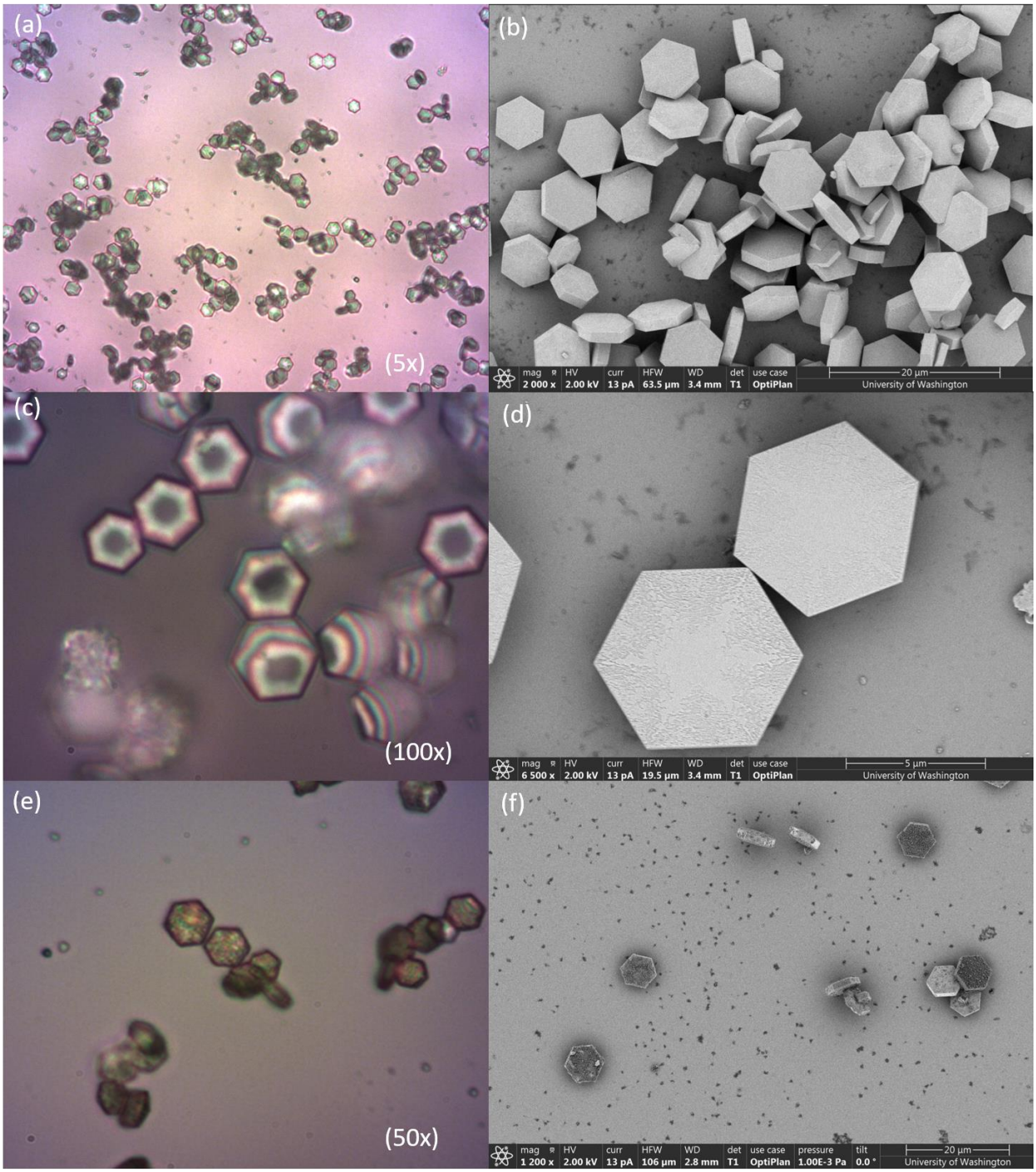

Figure 23. Light Microscopy and SEM images of (a-d) bulk β-NaYF, and (e, f) PDAG @ β-NaYF coatings after 72h hydrothermal synthesis of PDAG on the previously synthesized β-NaYF. Birefringent nature of the discs can be seen to diminish in (e) and darkened discs are shown in (f).

SEM Photo credit: Lars Forberger

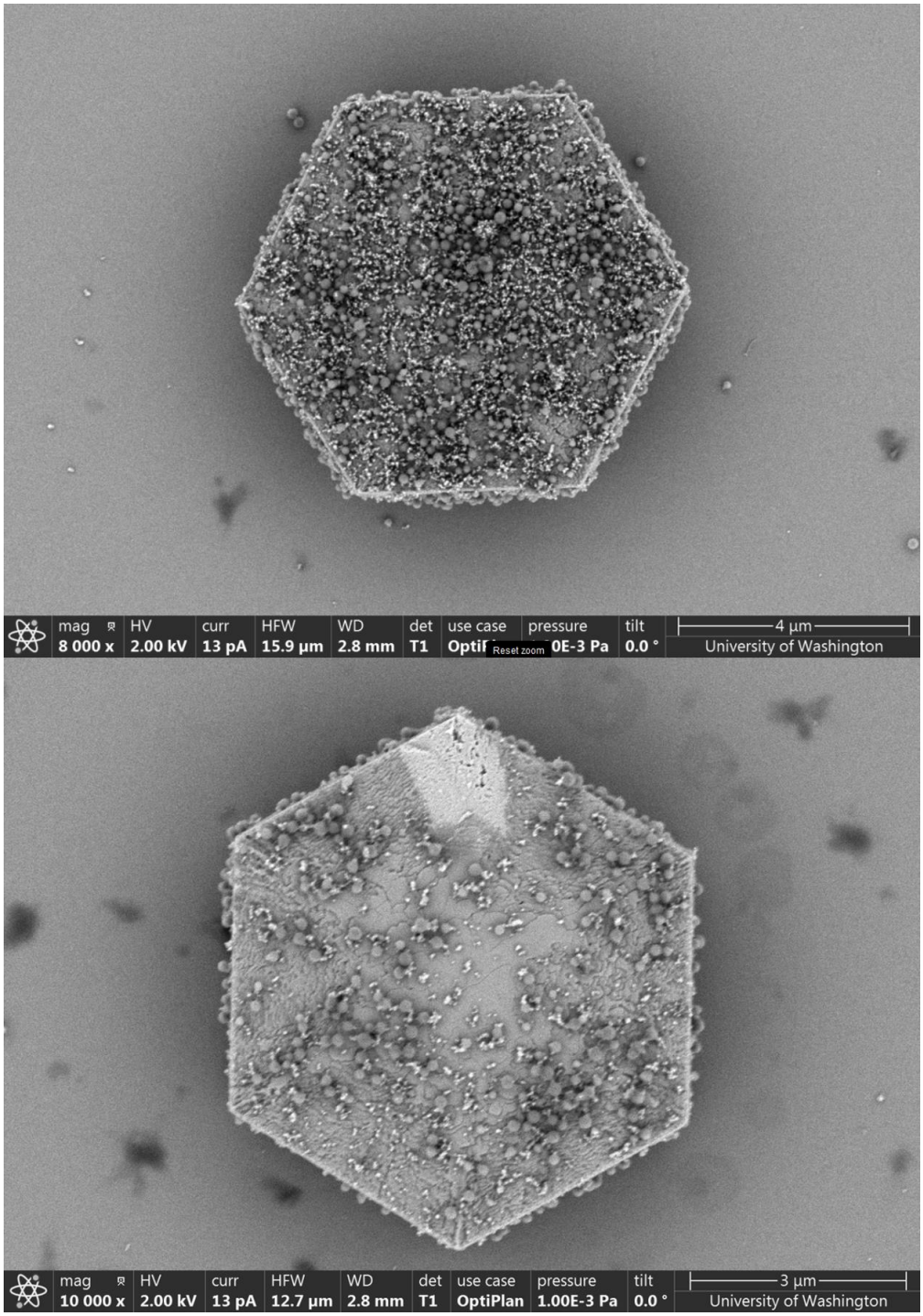

Figure 24. SEM images of PDAG @ β-NaYF showing full coverage and decoration (top) and significant coverage with mild decoration (bottom).

SEM Photo credit: Lars Forberger

2.2.8 Exposure of PDAG@β-NaYF to PBS and Enzyme Conjugation

Regrettably, only one attempt was able to be made to conjugate the enzyme to the PDAG surface. The purification was carried out by my colleague, Rachel Gariepy, while Lars Forberger prepared the sample for SEM images, shown in **Figure 25**. These PDAG@β-NaYF particles were exposed to PBS and the target enzyme for ~8 days before being purified. The sample was not accessed in time to test

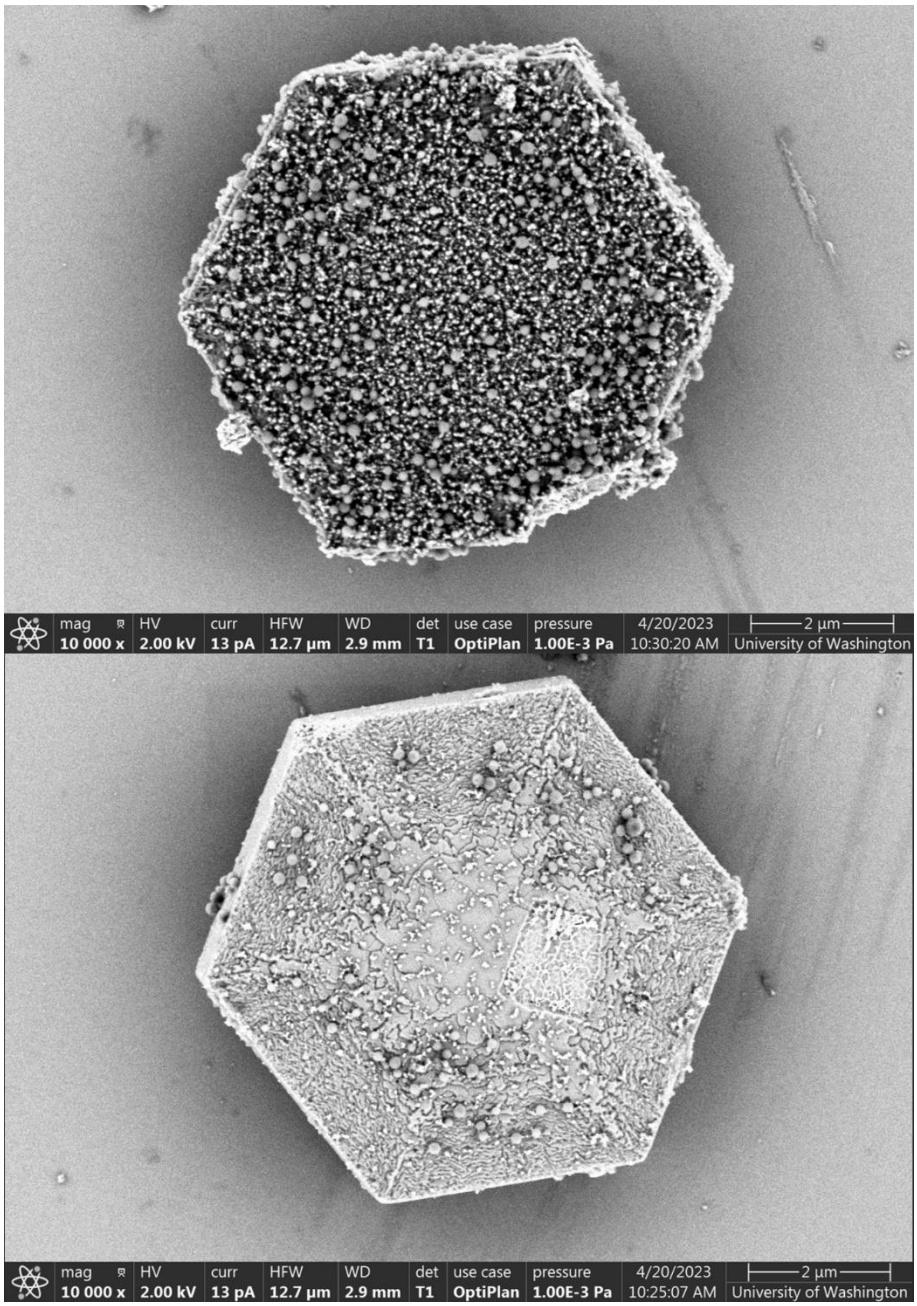

Figure 25. SEM Images of two different PDAG@β-NaYF particles after being (accidentally) exposed to PBS and the target enzyme for ~185 hours. The coatings appear to still be mostly intact and enzymatic activity may yet be possible.

Photo credit: Lars Forberger

it for enzymatic activity so this is the final project result for this thesis: a coat of polydopamine that has been extensively crosslinked by glutaraldehyde and appears to be nominally resistant to the majority of aggregation effects that PBS would otherwise cause in pure dopamine and dopamine-oligomer species.

2.2.9 PDA – Laser Trapping Results

Other results that are important to mention are the observed interactions that PDA has with the 1020nm laser being used to excite YLF. A significantly diluted sample of ~300nm PDANP was placed into the sample holder of the optical trap and PDANP were seen to “fly away” from the laser, only to later be found being essentially pushed up against the glass coverslip. In **Figure 26**, this mechanism can be seen where, when the laser is turned on, PDANP begin to aggregate as a fluid-like body within the optical trap. When the laser is turned off, the particles disperse into the local fluid volume. This can be repeated many times with the same result.

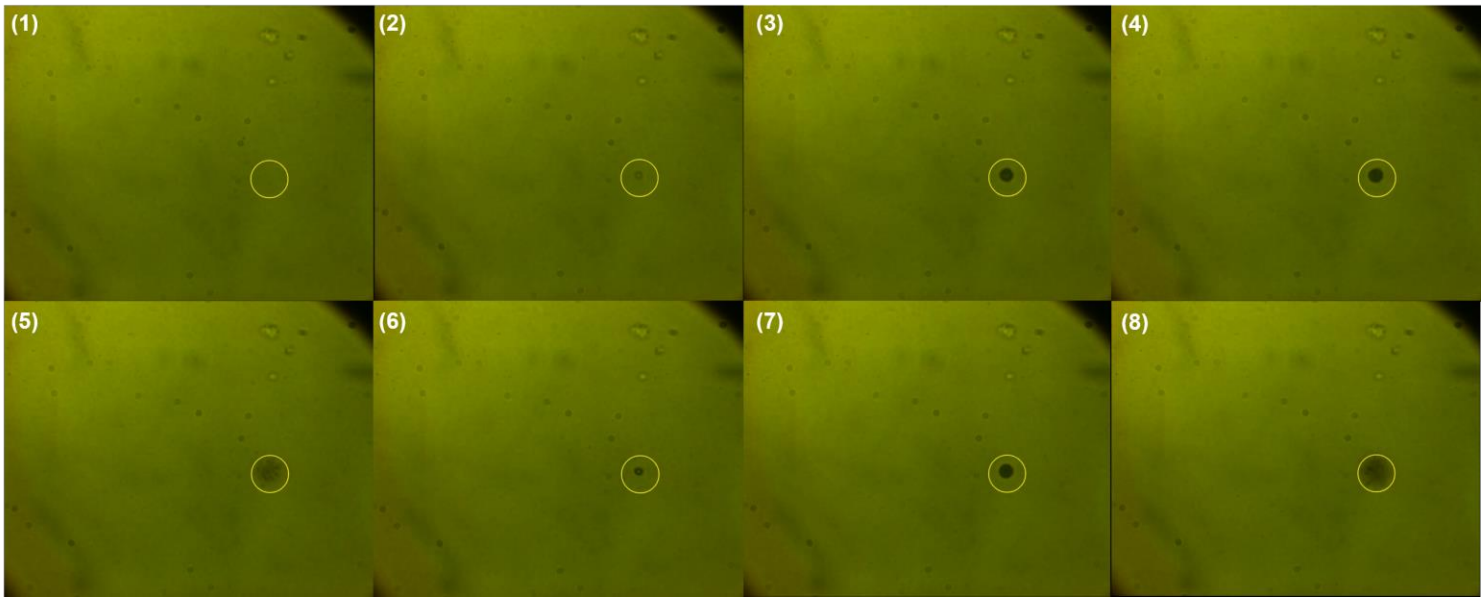

Figure 26. Still images of a video depicting the accretion of PDA from the local fluid volume (1) no particles in the trap. (2) the laser is switched on, some particles snap in. (3, 4) particles aggregate from the local volume. (5) the laser is turned off and particles scatter. (6, 7) the laser is turned on, particles aggregate. (8) the laser is turned off. Video capture credit: Rachel Gariepy

Approximately five minutes was spent playing a scavenging game around the sample, collecting as many particles in the trap as possible. This was done with the intent to study if the behavior can be replicated at a much grander scale. These results are displayed in **Figure 27**. In this figure, still images of the video were taken to illuminate how actively these particles aggregate when the laser is on, how much they disperse when the laser is off, and how densely these particles seek to pack themselves while being exposed to the laser.

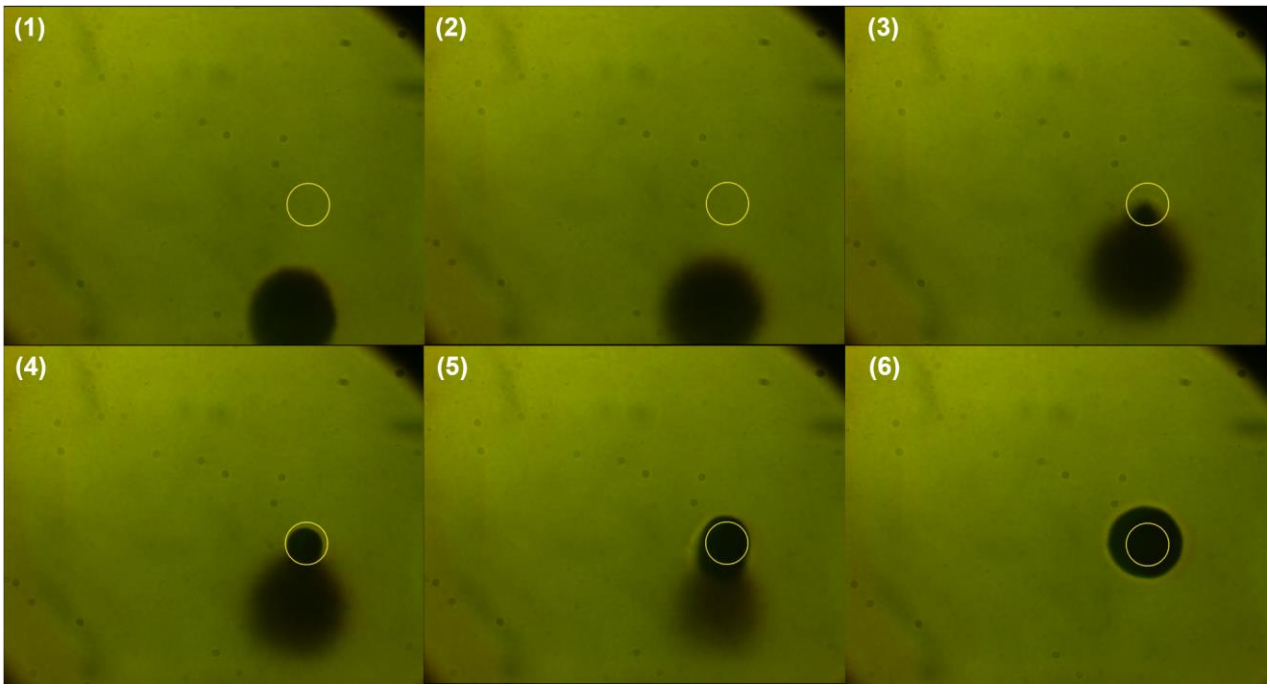

Figure 27. Still images of a video depicting the accretion of PDA from the local fluid volume (1) the laser is on but focused away from the yellow circle. PDANP continue to aggregate along the laser path. (2) the laser is switched off and refocused to the yellow circle while the particles begin to diffuse away from each other. (3) the laser is turned on. PDANP begins to pointedly flow into the trap and (4, 5) PDA visibly flows into the optical trap until (6) all of the local PDANPs are being held against the glass cover slip by the 1020nm laser.

2.2.10 PDAG – Laser Trapping Results

Interestingly, the hydrothermally-produced PDAG particles behave differently than PDA particles do. Upon being viewed in the same optical trap setup as PDANP, it is observed that they do not interact with the 1020nm laser in the same way. Though it may be an artifact of them being larger particles, they also do not interact with each other the same way as PDANP. Where PDANP can be repeatedly, controllably aggregated and dispersed, PDAGNP are slightly more difficult to hold in place. They do not actively flow into the trap as readily as PDANP, as can be seen in **Figure 28 (3-7)** as one particle is seen firmly departing from the optical trap despite the laser being on (the laser is off in frames (4) and (6)). This work bears repeating in a higher concentration setting or after PDAGNP synthesis has been optimized.

In the recorded video, considerable time was spent attempting to move a particle away from the glass coverslip but largely to no avail. These large PDAGNPs seemed to have a lower mobility compared to the much smaller PDANPs and their scarcity throughout the sample volume led to difficulty in preparing adequate footage for analysis. Time was also spent scavenging for particles but there was difficulty in coaxing them to all uniformly together and drag them around as a single unit.

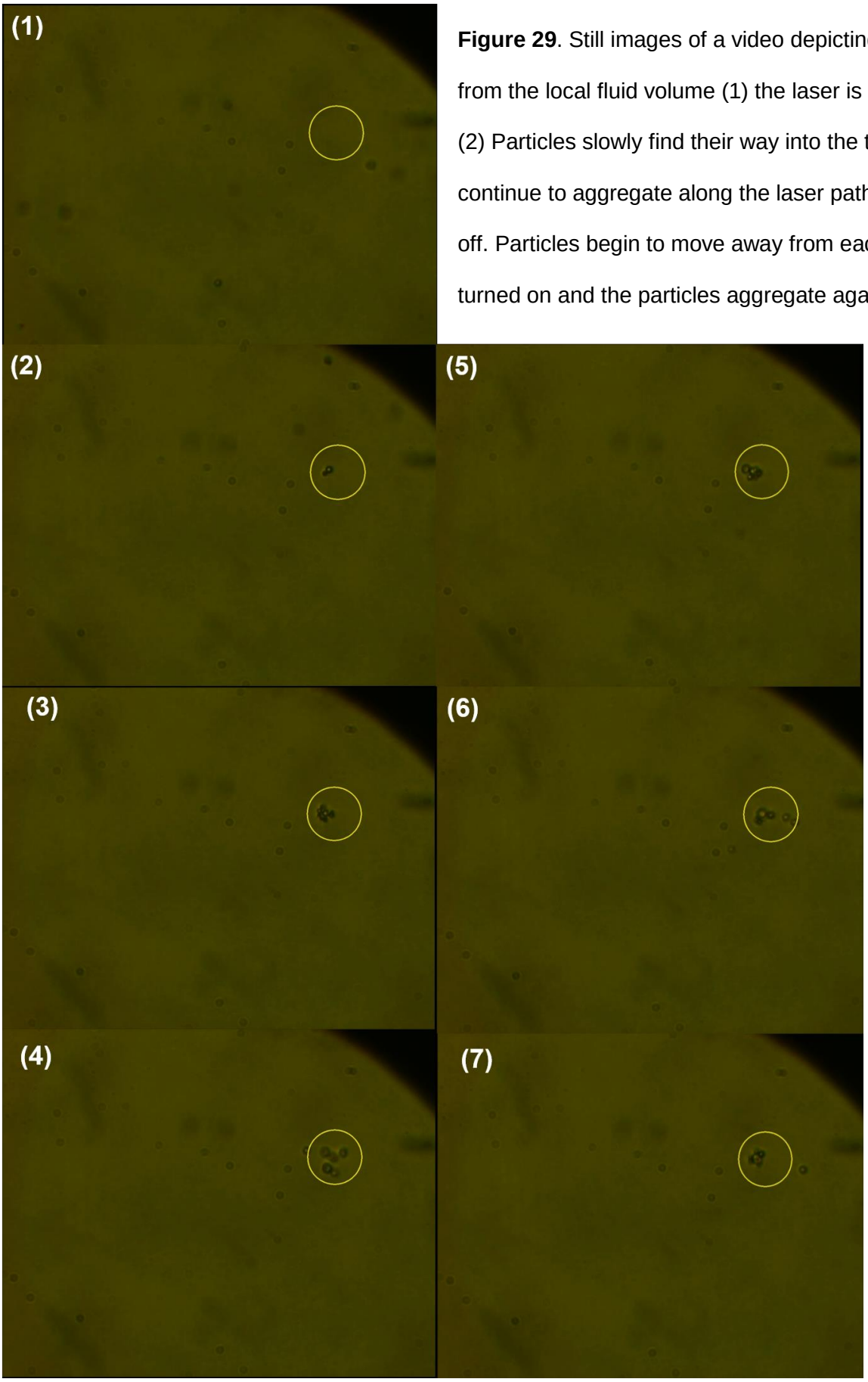

Figure 29. Still images of a video depicting the accretion of PDA from the local fluid volume (1) the laser is on and the trap is empty. (2) Particles slowly find their way into the trap and (3) PDAGNP continue to aggregate along the laser path. (4) the laser is switched off. Particles begin to move away from each other. (5) the laser is turned on and the particles aggregate again. (6) The laser is turned off and the particles move away from each other. (7) The laser is turned on and most particles aggregate into the trap again while one seems to continue moving away.

2.3 Discussion

2.3.1 PDA coatings over YLF

The PDA coating of YLF was performed in a gentle mixing method wherein the concentration of dopamine was constantly replenished. Because a film formed, there must be a chemical equilibrium term that favors film formation associated with an increase in monomer concentration. This is best understood using Le Châtelier's Principle: with the typical synthesis product being relatively monodisperse spheres, an excess addition of monomer dramatically moves the equilibrium to favor the initiation and elongation of films along the ceramic substrate. With gentle fluid mixing, this could be an effective method of simultaneously coating many fragile ceramic particles if hydrothermal temperature and pressure is not a viable option.

Although this PDA layer has the characteristic of significantly heating in response to 980nm, it could not be usable for studying the laser cooling at 1020nm. However, because YLF has a laser heating response at 980nm, it is possible that these heating modes may be coupled together and enable the development of composite materials that can be precisely laser heated to achieve highly specific or sensitive temperature profiles.

Because the layer of polydopamine still maintains enough chemical reactivity to be polymerized, it is possible that a smoother, more uniform PDA coating could be efficiently decorated with various types of materials including entirely other ceramic materials, superparamagnetic nanomaterials, or nanomaterials that have an optical response/surface plasmon resonance. The development of composite structures with symbiotic multifunction is an exciting space to develop into.

2.3.2 PDA in One Dimension

Although receiving only a small mention in *Section 2.2.4.1*, it is worth discussing the plausibility of single-dimensional PDA wire structures that possibly formed in the attempt to use dopamine as a stabilizing surfactant in YLF synthesis. As a side note, since it was only attempted the one time, it is not reasonable to completely discount that there may be something worth studying between nucleating

YLF and lower concentrations of dopamine present in the solution. It is suspected that at lower concentrations, it is possible that dopamine may participate with YLF crystals in some way because it would not have the chemical potential to form poly/oligomeric species and undesirably nucleate into particles.

It is believed that **Figure 20** is the product of a high ionic strength solution. Conducting studies using NH_4Cl would be a useful way of testing this. Depending on the durability of the materials *in situ*, a stirred autoclave may be used. However, it is also possible that using a stirred autoclave will result in a more spherical or amorphous aggregate morphology due to shear forces (this would be based on the stir bar rotation speed).

2.3.3 PDAG Films, Nanoparticles, and Coating Formation

The mechanism of PDAG film formation is a crosslinking via condensation, forming imines from the primary amines of dopamine and its oligomers. The PDAG products obtained- little X's, films of increasing thickness and durability, spherical particles, and coatings, display a versatility to this polymer species not typically expected from glutaraldehyde (which is expected to rigidify structures and shut down their reactivity [18]). Without mechanical input, it forms as little X's. When stirred, it appears to form thin films. When heated and pressurized, it forms particles and, in the presence of a ceramic surface, preferentially deposits upon it.

PDAG is a material worth investing time in studying because of the possibility that the absorption wavelength has shifted into the UV is, considering the color of the GA v/v% experiments. If this wavelength has truly shifted away from ~1020nm, it would open up many doors for studying anything that could be stuck to the surface and possibly cooling it radiatively due to β-NaYF photonic upconversion at 1020nm. This is a monumental issue because PDA has been found to have a remarkable heating effect in this region and can be used as a thermal ablation cancer therapy mode.

It would be preferable to develop a method by which the formation of the PDAG coat on a surface can be qualified without the need for SEM imaging. UV-Vis would be an effective method of attempting

this as the PDAG film synthesis fluid produced a fluid that seemed to absorb around 400nm. FTIR is another possible avenue to achieve this by possibly exploring a lowering trend in the number of functional groups as the degree of polymerization is increased.

Additionally, PDAG deposition likely proceeds at a much more rapid rate at high temperature and pressure than the allotted 72h. It would be beneficial to test the coating mechanism with 1, 2, 4, and 8h syntheses (and repeat with varying reaction parameters) to see what kind of film product forms. It would be ideal to produce a uniform PDAG thin film in a short timeframe that was not decorated with so many visually congesting particles. This timed termination may lead to a truncated crosslinking mechanism, yielding different surface chemistry, depending on how many crosslinking agents were present in the initial reaction and how far to t_∞ it was allowed to complete. Expanding the study into the different GA v/v% could help to discern a more ideal concentration of glutaraldehyde or dopamine for producing thinner/thicker coats- possibly even more rapidly.

In the scope of conjugating an enzyme to the surface of PDAG, understanding the planned termination outlined above may be critical because certain enzymes, such as horseradish peroxidase, participate in an extremely rapid oxidation of dopamine to eumelanin aggregates in the presence of H_2O_2. [21] Once it has been confirmed that an enzyme has been conjugated to the PDAG surface, it may be necessary to backfill any remaining reactive sites with BSA (bovine serum albumin), for example, to passivate the surface without interfering with the enzyme reactivity. If this is possible without interfering with the optical activity of the crystal, this would be an effective method of studying enzyme rate kinetics based on laser-induced mechanisms as it would provide the PDAG surface with resistance to enzymatic attack.

In the same vein as resistance to enzyme degradation, because this PDAG surface was incidentally found to be present even after ~8 days in PBS, it is possible that further study could produce a material that is decently resistant to saline solutions. This may confer corrosion resistance to materials that can withstand the hydrothermal synthesis parameters of PDAG coating (although these should currently be up for adaptation and optimization).

2.3.4 Optical Trapping of PDANPs vs. PDAGNPs

When the 1020nm laser of the optical trap is off, an aggregated cloud of PDANPS is observed to diffuse over time into the extended local fluid volume. When the laser is turned on, these particles do not suddenly and instantaneously transport into the trap and, instead, flow into the optical trap at an observable rate. Based on the way the cloud appears to "point" in **Figure 27(3)** and the definition of the condensed cloud in part (4), the rate at which this material enters the trap may be based on the width of the beam and the power of the laser. In **Figure 27(5, 6)**, the aggregate cloud is seen to have grown and exceeded what the laser can stably hold against the glass coverslip. In other frames of the video (not shown), as the laser is moved, the aggregate cloud "shakes" off a portion of itself as the particles move in conjunction with the laser. These shaken off PDANPs immediately fall back into the cloud being held in place by the laser. This can be done quite quickly and the PDANP spot will follow the laser. It is possible that these particles may be able to be "flung" by dragging the laser in the XY-plane and shutting it off, giving the PDANPs a velocity. Only the footage of the PDAGNPs had the laser power recorded at ~45mW so a more systematic study of the possible motive ability of PDANP would need to be conducted to see if there is any correlation between laser power, laser wavelength, and aggregation/dispersion mechanism.

PDAGNPs have a slightly different behavior in the 1020nm optical trap. Perhaps because they are more dense/massive or the particle density of the sample was low, but they appeared much slower to respond to the optical trap, overall. That being said, they appeared to have a different optical characteristic compared to the PDANPs. This could be beneficial to optimize and study by attempting a synthesis of monodisperse, <500nm diameter PDAGNPs in a stirred autoclave and adding a higher concentration of the sample to the sample holder.

3. Conclusion & Future Work

3.1 Conclusions

In conclusion, two different methods of coating rare earth-doped (RE) ceramic materials with polydopamine were outlined. The first grows a dopamine coating by constantly replenishing the dopamine monomer concentration under gentle mixing. This coating is largely subject to chemical modification by PBS and, essentially, removal by glutaraldehyde. Based on qualitative assays (not shown), even the aggregated polymer seemed to maintain some amount of enzyme reactivity after attempted conjugation.

The condensation polymerization reaction between glutaraldehyde and dopamine forms macroscopic structures that can be hydrothermally grown as a coating on the surfaces of previously synthesized RE ceramics. This coating is resistant to PBS and its growth may be able to be optimized to develop a surface that is multifunctional, stable, and possibly biocompatible.

One-dimensional, polymeric materials that could possess the many properties of polydopamine may possibly be grown in ionic solution. It is possible they could be used for developing soft polymer wires or coils to build structures that can exist stably in aqueous environments and be locally heated in response to near-IR and IR wavelengths of light. If thin, single wires could be grown and isolated, they should be tested for paramagnetism [13], laser heating, and what sort of surface chemistry it possesses.

PDANPs and PDAGNPs both respond to high powered laser light by flowing into the optical trap at an observable rate that could potentially be measured. The nanoparticles formed from PDAG behaved and appeared differently than PDANP in the same optical trap- indicating some variation in their surface charge. It may be useful to develop similar samples of these two materials for studying Brownian motion and if PDAGNPs continue to laser heat in the near-IR and IR.

3.2 Future Work

Because PDANP are known to laser heat at broadly around 980nm and 1020nm, it should be explored if PDAGNP respond similarly, as well as surfaces coated by it. Analyzing the PDAG surface to

understand its chemical, physical, and mechanical differences from PDA would serve good purpose in planning an optimization of the coat and coating process. Theoretically, it should be possible to develop PDAG into a bifunctional surface that can readily adhere to substrates and make anchoring of delicate objects a much simpler process.

Optimizing the PDA coating process of YLF crystals to explore their usage in optically neutral plastics. Theoretically, exposing a composite plastic such as this should generate a spike in heat. If molding a 96-well plate using the embedded plastic and exposing it to 980nm produces a quantifiable temperature profile, it would be possible to determine the duration and power of laser light necessary to supply a thermal “dose” and locally heat all 96 wells. This laser heating could potentially replace convection heating.

Principally, more study needs to be conducted as to how effective the conjugation of enzymes to the PDAG surface is. A polymeric material that is strongly adhesive but optically neutral in the desired region of study is an ideal case. Beyond just enzymatic study, purposefully coating fragile ceramic microcrystals in PDAG may confer them a greater lifetime for various applications due to the structural support. At the same time, more effective methods need to be used to qualify that the formed PDAG has been successfully crosslinked to the desired level. It is possible that FTIR could be used to indicate the difference in the signal reduction of primary amines between PDANP and an exploration of PDAGNP/PDAG-coated materials. If a correlation can be found here, a robust coating of PDAG may be experimentally derived and applied ubiquitously to a broad range of ceramic materials.

Other considerations made during the scope of this work included that PDA materials can be pyrolyzed into N-doped graphene materials, shown in **Figure 29**. [6] If it is possible to maintain the geometry during the pyrolyzation (or possibly carbonization using H_2SO_4), these N-doped graphene NPs could be put into a diamond anvil cell and diamond nanoparticles with embedded NV^- centers may be viable.

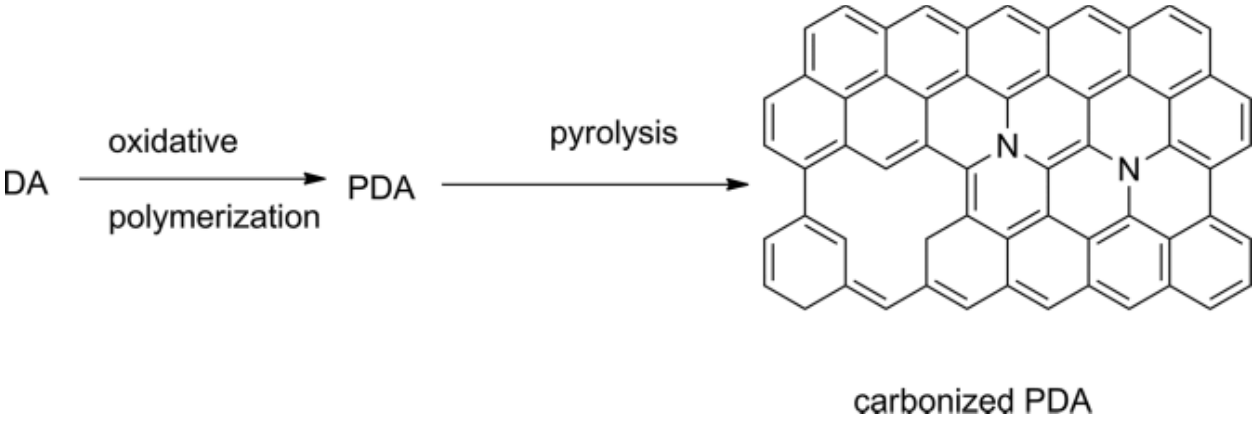

Figure 29. Pyrolysis of PDA materials into N-doped, graphenic materials. [6]

Acknowledgements

Paul C. Painter and Michael M. Coleman for writing Fundamentals of Polymer Science.

Dr. Pauzauskie

Dr. Roumeli

My cat

Pauzauskie Group:

Alex Bard Alexey Soldatenko Andy Feng Christopher Woodburn

Lars Forberger Rachel Gariepy Chaman Gupta Michael Hilyard

Sankhya Hirani

References

[1] Lee, H., Dellatore, S. M., Miller, W. M., & Messersmith, P. B. (2007). Mussel-Inspired Surface Chemistry for Multifunctional Coatings. *Science*, *318*(5849), 426–430. https://doi.org/10.1126/science.1147241

[2] Almeida, L., Correia, R. N., Marta, A., Squillaci, G., Morana, A., Francesco La Cara, Correia, J., & Luiza, A. (2019). Electrosynthesis of polydopamine films - tailored matrices for laccase-based biosensors. *Applied Surface Science*, *480*(480), 979–989. https://doi.org/10.1016/j.apsusc.2019.03.015

[3] Liu, Y., Ai, K., & Lu, L. (2014). Polydopamine and Its Derivative Materials: Synthesis and Promising Applications in Energy, Environmental, and Biomedical Fields. *Chemical Reviews*, *114*(9), 5057–5115. https://doi.org/10.1021/cr400407a

[4] Liu, Y., Ai, K., Liu, J., Deng, M., He, Y., & Lu, L. (2012). Dopamine-Melanin Colloidal Nanospheres: An Efficient Near-Infrared Photothermal Therapeutic Agent for In Vivo Cancer Therapy. *Advanced Materials*, *25*(9), 1353–1359. https://doi.org/10.1002/adma.201204683

[5] B. Kollbe Ahn. (2017). Perspectives on Mussel-Inspired Wet Adhesion. *Journal of the American Chemical Society*, *139*(30), 10166–10171. https://doi.org/10.1021/jacs.6b13149

[6] Liebscher, J. (2019). Chemistry of Polydopamine - Scope, Variation, and Limitation. *European Journal of Organic Chemistry*, *2019*(31-32), 4976–4994. https://doi.org/10.1002/ejoc.201900445

[7] Karlsson, O., & Nils Gunnar Lindquist. (2016). Melanin and neuromelanin binding of drugs and chemicals: toxicological implications. *Archives of Toxicology*, *90*(8), 1883–1891. https://doi.org/10.1007/s00204-016-1757-0

[8] Watt, A. A. R., Bothma, J. P., & Meredith, P. (2009). The supramolecular structure of melanin. *Soft Matter*, *5*(19), 3754. https://doi.org/10.1039/b902507c

[9] Alfieri, M. L., Micillo, R., Panzella, L., Crescenzi, O., Oscurato, S. L., Maddalena, P., Napolitano, A., Ball, V., & d'Ischia, M. (2017). Structural Basis of Polydopamine Film Formation: Probing 5,6-

Dihydroxyindole-Based Eumelanin Type Units and the Porphyrin Issue. *ACS Applied Materials & Interfaces*, *10*(9), 7670–7680. https://doi.org/10.1021/acsami.7b09662

[10] Lynge, M. E., Westen, R. van der, Postma, A., & Städler, B. (2011). Polydopamine—a nature-inspired polymer coating for biomedical science. *Nanoscale*, *3*(12), 4916–4928. https://doi.org/10.1039/C1NR10969C

[11] Li, Z., Zhang, X., Wang, S., Yang, Y., Qin, B., Wang, K., Xie, T., Wei, Y., & Ji, Y. (2016). Polydopamine coated shape memory polymer: enabling light triggered shape recovery, light controlled shape reprogramming and surface functionalization. *Chemical Science*, *7*(7), 4741–4747. https://doi.org/10.1039/C6SC00584E

[12] Liao, M., Wan, P., Wen, J., Gong, M., Wu, X., Wang, Y., Shi, R., & Zhang, L. (2017). Wearable, Healable, and Adhesive Epidermal Sensors Assembled from Mussel-Inspired Conductive Hybrid Hydrogel Framework. *Advanced Functional Materials*, *27*(48), 1703852. https://doi.org/10.1002/adfm.201703852

[13] Fyodor, N., Luchini, A., Napolitano, A., Gerardino D'Errico, Vitiello, G., Szekely, N., d'Ischia, M., & Paduano, L. (2014). Tris Buffer Modulates Polydopamine Growth, Aggregation, and Paramagnetic Properties. *ACS Publications*, *30*(32), 9811–9818. https://doi.org/10.1021/la501560z

[14] Li, H., Xi, J., Donaghue, A. G., Keum, J., Zhao, Y., An, K., McKenzie, E. R., & Ren, F. (2020). Synthesis and catalytic performance of polydopamine supported metal nanoparticles. *Scientific Reports*, *10*(1). https://doi.org/10.1038/s41598-020-67458-9

[15] Arroquia, A., Acosta, I., & Armada, M. P. G. (2020). Self-assembled gold decorated polydopamine nanospheres as electrochemical sensor for simultaneous determination of ascorbic acid, dopamine, uric acid and tryptophan. *Materials Science and Engineering: C*, *109*(110602). https://doi.org/10.1016/j.msec.2019.110602

[16] Zou, Y., Chen, X., Yang, P., Liang, G., Yang, Y., Gu, Z., & Li, Y. (2020). Regulating the absorption spectrum of polydopamine. *Science Advances*, *6*(36). https://doi.org/10.1126/sciadv.abb4696

[17] Painter, P. C., & Coleman, M. C. (1997). *Fundamentals of Polymer Science, An Introductory Text* (2nd ed.). The Pennsylvania State University. (Original work published 1997)

[18] Uhr, H., Mielke, B., Exner, O., Payne, K. R., & Hill, E. (2013). Biocides. *Ullmann's Encyclopedia of Industrial Chemistry*, 1–26. https://doi.org/10.1002/14356007.a16_563.pub2

[19] d'Ischia, M., Napolitano, A., Pezzella, A., Meredith, P., & Sarna, T. (2009). Chemical and Structural Diversity in Eumelanins: Unexplored Bio-Optoelectronic Materials. *Angewandte Chemie International Edition*, *48*(22), 3914–3921. https://doi.org/10.1002/anie.200803786

[20] Zhou, J., Duan, B., Fang, Z., Song, J., Wang, C., Messersmith, P. B., & Duan, H. (2013). Interfacial Assembly of Mussel-Inspired Au@Ag@ Polydopamine Core-Shell Nanoparticles for Recyclable Nanocatalysts. *Advanced Materials*, *26*(5), 701–705. https://doi.org/10.1002/adma.201303032

[21] Li, J., Baird, M. A., Davis, M. A., Tai, W., Zweifel, L. S., Waldorf, K. M. A., Gale Jr, M., Rajagopal, L., Pierce, R. H., & Gao, X. (2017). Dramatic enhancement of the detection limits of bioassays via ultrafast deposition of polydopamine. *Nature Biomedical Engineering*, *1*(6), 1–12. https://doi.org/10.1038/s41551-017-0082

[22] Malollari, K. G., Peyman Delparastan, Sobek, C., Vachhani, S. J., Fink, T. D., R. Helen Zha, & Messersmith, P. B. (2019). Mechanical Enhancement of Bioinspired Polydopamine Nanocoatings. *Applied Materials & Interfaces*, *11*(46), 43599–43607. https://doi.org/10.1021/acsami.9b15740

[23] Li, Z., Yang, Y., Wang, Z., Zhang, X., Chen, Q., Qian, X., Liu, N., Wei, Y., & Ji, Y. (2017). Polydopamine nanoparticles doped in liquid crystal elastomers for producing dynamic 3D structures. *Journal of Materials Chemistry A*, *5*(14), 6740–6746. https://doi.org/10.1039/C7TA00458C

[24] Nam, H. J., Cha, J., Lee, S. H., Yoo, W. J., & Jung, D.-Y. (2014). A new mussel-inspired polydopamine phototransistor with high photosensitivity: signal amplification and light-controlled switching properties. *Chemical Communications*, *50*(12), 1458–1461. https://doi.org/10.1039/C3CC48309F

[25] Kim, Y., Coy, E., Kim, H., Mrówczyński, R., Torruella, P., Jeong, D.-W., Choi, K. S., Jang, J. H., Song, M. Y., Jang, D.-J., Peiro, F., Jurga, S., & Kim, H. J. (2021). Efficient photocatalytic production of hydrogen by exploiting the polydopamine-semiconductor interface. *Applied Catalysis B: Environmental*, *280*, 119423. https://doi.org/10.1016/j.apcatb.2020.119423

[26] Jiang, Y., Lan, Y., Yin, X., Yang, H., Cui, J., Zhu, T., & Li, G. (2013). Polydopamine-based photonic crystal structures. *Journal of Materials Chemistry C*, *1*(38), 6136. https://doi.org/10.1039/c3tc30114a

[27] Han, Y., Zhu, Z., Huang, L., Guo, Y., Zhai, Y., & Dong, S. (2019). Hydrothermal synthesis of polydopamine-functionalized cobalt-doped lanthanum nickelate perovskite nanorods for efficient water oxidation in alkaline solution. *Nanoscale*, *11*(41), 19579–19585. https://doi.org/10.1039/C9NR06519A

[28] Zhang, X., Ceccarelli, M., Deng, F., Huang, H., Wan, Q., Liu, M., & Wei, Y. (2017). Mussel-inspired fabrication of functional materials and their environmental applications: Progress and prospects. *Applied Materials Today*, *7*, 222–238. https://doi.org/10.1016/j.apmt.2017.04.001

[29] Liu, Y., Su, C., Zu, Y., Chen, X., Sha, J., & Dai, J. (2022). Ultrafast deposition of polydopamine for high-performance fiber-reinforced high-temperature ceramic composites. *Scientific Reports*, *12*(1), 20489. https://doi.org/10.1038/s41598-022-24971-3